RESEARCH ARTICLE

AMERICAN JOURNAL OF BIOLOGICAL ANTHROPOLOGY
The Official Journal of the American Association of Biological Anthropologists

WILEY

Linking the proximal tibiofibular joint to hominid locomotion: A morphometric study of extant species

Annalisa Pietrobelli[1] | Rita Sorrentino[1,2] | Stefano Benazzi[2] | Maria Giovanna Belcastro[1] | Damiano Marchi[3,4]

[1]Department of Biological, Geological and Environmental Sciences, University of Bologna, Bologna, Italy

[2]Department of Cultural Heritage, University of Bologna, Ravenna, Italy

[3]Department of Biology, University of Pisa, Pisa, Italy

[4]Centre for the Exploration of the Deep Human Journey, University of the Witwatersrand, Johannesburg, South Africa

Correspondence
Annalisa Pietrobelli, Department of Biological, Geological and Environmental Sciences, University of Bologna, Bologna, Italy.
Email: annalisa.pietrobell2@unibo.it

Damiano Marchi, Department of Biology, University of Pisa, Pisa, Italy.
Email: damiano.marchi@unipi.it

Abstract

Objectives: We perform a comparative assessment of shape variation of the proximal fibula in extant humans and great apes, intending to investigate the possible link between proximal fibular shape and locomotor patterns.

Methods: Our sample includes 94 fibulae of 37 *Homo sapiens*, 15 *Gorilla*, 17 *Pongo*, and 25 *Pan*. Fibular morphology was investigated through three-dimensional (semi) landmark-based geometric morphometric methods.

Results: We found unique features of the human fibular head compared to that of great apes (i.e., oblique articular surface, the presence of the styloid process, specific morphology of muscle attachment sites), supporting the functional role of this bone in relation to human obligate bipedalism. Great apes also showed distinctive traits in their proximal fibula morphology, in agreement with differences in locomotor behavior.

Conclusion: The morphology of the proximal fibula in extant humans and great apes is indicative of locomotor behavior, offering the potential for the comparative analysis of fossil hominin remains.

KEYWORDS
3D geometric morphometrics, bipedalism, fibula, functional morphology, great apes

1 | INTRODUCTION

Obligate bipedalism and upright posture are considered characteristic traits of *Homo sapiens*, which is a fully terrestrial biped (Aiello & Dean, 1990; Harcourt-Smith, 2015; Harcourt-Smith & Aiello, 2004). On the other hand, *Pan* and *Gorilla* frequently engage in terrestrial quadrupedalism (about 85%–95% of their locomotor behavior; Carlson, 2005; Doran, 1996), mostly knuckle-walking/running. Less than about 1.5% of *Pan* locomotor and postural repertoire is dedicated to

terrestrial/arboreal bipedalism (Carlson, 2005; Crompton et al., 2010). *Pan* genus engages in frequent (about 8%–18%) arboreal locomotion (Carlson, 2005; Doran, 1993, 1996), with about 56% arboreal positional behaviors dedicated to vertical climbing/descent (Crompton et al., 2010) and about 11%–44% dedicated to arboreal quadrupedalism (Doran, 1996). Indeed, most studies agree that gorillas are less arboreal than chimpanzees and bonobos (Crompton et al., 2010; Doran, 1996; Tuttle & Watts, 1985). Mountain gorillas are usually considered the least arboreal of all the great apes since they primarily engage in terrestrial quadrupedalism (Remis, 1995). They spend less than 1% of total locomotor time engaging in vertical climbing (avoiding terminal branches and in closeness to the center of the tree),

2 | WILEY AMERICAN JOURNAL OF BIOLOGICAL ANTHROPOLOGY The Official Journal of the American Association of Biological Anthropologists

PIETROBELLI ET AL.

mainly performed by females and juveniles (Remis, 1995; Tuttle & Watts, 1985). Both mountain and lowland gorillas engage in terrestrial and arboreal scrambling (Remis, 1995; Tuttle & Watts, 1985). In contrast to mountain gorillas, western lowland gorillas climb considerably more often (Doran & NcNeilage, 1993; Remis, 1995, 1998). Gorillas also engage in either terrestrial or arboreal bipedal locomotion (1%–6%, Tuttle & Watts, 1985; Remis, 1995; Crompton et al., 2010). Orangutan locomotor activity is mainly restricted to the canopy (Thorpe & Crompton, 2006). Although slight differences in positional behaviors among the species of orangutans are present, the kind of arboreal locomotion employed by the two species does not vary much. The locomotor behavior of this taxon typically involves forelimb suspension with the trunk in orthograde posture and the hindlimb loaded in compression (35%) (Thorpe & Crompton, 2006) and vertical climbing/descent (about 25%–33%) (Cant, 1987; Manduell et al., 2012; Thorpe & Crompton, 2006). Orangutans also engage in bipedalism more frequently (7%) than other nonhuman great apes in arboreal settings and with extended hindlimbs (Thorpe et al., 2007). Various morphological traits in the lower limb are associated with bipedalism in humans, among which derived knee, and ankle joints that effectively stabilize the leg and foot during walking are hallmarks (DeSilva, 2008, 2009; Javois et al., 2009; Sylvester, 2013; Sylvester & Pfisterer, 2012; Tardieu, 1999).

The traits of the human knee mainly associated with bipedalism are the *valgus* position, a mechanism for patellar retention due to the elevation of the lateral condylar lip, anteroposterior elongation, and changes in the form of both tibial and femoral condyles that provide tibial dominance and an increased patellar moment arm, and an increased tibial cartilage contact derived by both genomic and epigenetic mechanisms (Frelat et al., 2017; Javois et al., 2009; Lovejoy, 2007; Tardieu, 1981, 1999). By contrast, great apes show abducted knees and asymmetrical femoral and tibial condyles with a relatively expanded medial condyle, transmitting more load through the medial compartment of the knee and an increased knee joint mobility determined by reduced femoral-tibial contact (Frelat et al., 2017; Sylvester, 2013; Sylvester & Pfisterer, 2012; Tardieu, 1999).

The human talocrural joint has a squared shape, which uniformly distributes forces across the joint, while in great apes, the joint is trapezoidal to accommodate the foot in extreme dorsiflexion during climbing (DeSilva, 2008, 2009, 2010; DeSilva & Throckmorton, 2010; Venkataraman et al., 2013). The talocrural joint faces inferiorly in modern humans, roughly perpendicular to the long axis of the tibial shaft, with an anterior tilt of the talocrural surface that allows a considerable degree of dorsiflexion that is required during bipedal locomotion (DeSilva, 2009; Latimer et al., 1987; Sorrentino, Carlson, et al., 2020; Sorrentino, Stephens, et al., 2020 Turley et al., 2015). Previous studies of the knee and ankle joints focused mainly on the femur, tibia, and talus (e.g., Frelat et al., 2017; Harmon, 2006, 2007, 2009; Sorrentino, Carlson, et al., 2020; Sorrentino, Stephens, et al., 2020) while the fibula has been generally overlooked. However, several studies have shown that fibular morphology is linked to locomotor behavior in mammals (Barnett & Napier, 1953; Carleton, 1941). Furthermore, in modern humans and primates, the degree of mobility of

the fibula has been related to the degree of eversion/inversion and dorsiflexion/plantarflexion at the ankle joint (Barnett & Napier, 1953). Among focusing on the lower limb in humans and fossil hominins Mary W. Marzke (e.g., Marzke et al., 1988; Nagano et al., 2005), to whom this Special Issue is dedicated, the study of McLean and Marzke (1994) was the first to report variations in fibular cortical thickness among chimpanzees and humans. In addition, recent studies conducted on the relative robusticity (as evidenced by cross-sectional geometry analysis) of the human and nonhuman primate fibula found a relationship between fibula/tibia diaphyseal strength ratios and degree of arboreal locomotion. More arboreal species were characterized by relatively more robust fibulae than terrestrial ones (Marchi, 2007, 2015a). It was proposed that this relationship may reflect the different degree of mobility of the fibula at the ankle joint due to the different range of foot dorsiflexion/plantarflexion and inversion/eversion generated during locomotion using arboreal vs. terrestrial substrates (Barnett & Napier, 1953; Carleton, 1941; DeSilva, 2009; Latimer et al., 1987; Stern & Susman, 1983).

Despite recent studies showing the importance of studying fibular diaphyseal strength to further our understanding of the degree of arborealism of early hominins (Marchi et al., 2019), less is known about the morphology of the proximal and distal ends. Concerning the distal end, previous studies performed using traditional morphometrics showed that great apes possess a more anteriorly oriented lateral malleolus and more downward facing fibulo-talar articular facets as well as a more craniocaudally elongated subcutaneous triangular surface (STS) than humans (Marchi, 2015b; Stern & Susman, 1983). A recent 3D geometric morphometric (3D-GM) study revealed that the distal fibular morphology indicates arboreal vs. terrestrial locomotor patterns within extant hominids (Marchi et al., 2022). The study confirms and expands previous morphological observations regarding the orientation of the lateral malleolus, fibulotalar articular facets, and STS proportions, implying a wider peroneal groove and a deeper and broader malleolar fossa in great apes than in humans. On the other hand, the proximal fibular epiphysis is rarely investigated in humans except for clinical purposes, and even less data are available for great apes.

1.1 | Anatomy and biomechanics of the proximal fibula and proximal tibiofibular joint in modern humans

The proximal fibula (Figure 1, Figure S1) in modern humans is composed of the fibular head, a mediolaterally expanded bone protrusion surmounting the fibular neck and accommodating the proximal tibiofibular articular surface (Martini et al., 2009). The proximal extremity of the fibular head bears the styloid process, serving as the insertion for the popliteofibular tendon (PFT). At the same time, a lateral bulge holds the insertion area for the *m. biceps femoris* (knee flexor) tendon (BT) and the fibular collateral ligament (FCL; Song et al., 2018, 2020; Takahashi et al., 2017).

The anatomy of the proximal tibiofibular joint (PTFJ) is a plane synovial joint between the articular facet on the lateral condyle of the

PIETROBELLI ET AL.

AMERICAN JOURNAL OF
BIOLOGICAL ANTHROPOLOGY
The Official Journal of the American Association of Biological Anthropologists

WILEY

3

FIGURE 1 Landmark configuration on a human left proximal fibula. (a) Proximal view, (b) anterolateral view and right, (c) posteromedial view. Black dots are fixed landmarks, light blue dots are curve semilandmarks and orange dots are surface semilandmarks. (d) curve "a" definition on a human left proximal fibula, proximal view. See Table 2 for definition of numbered landmarks and curve. EpSur = epiphyseal surface; TFHSur = tibiofibular articular surface.
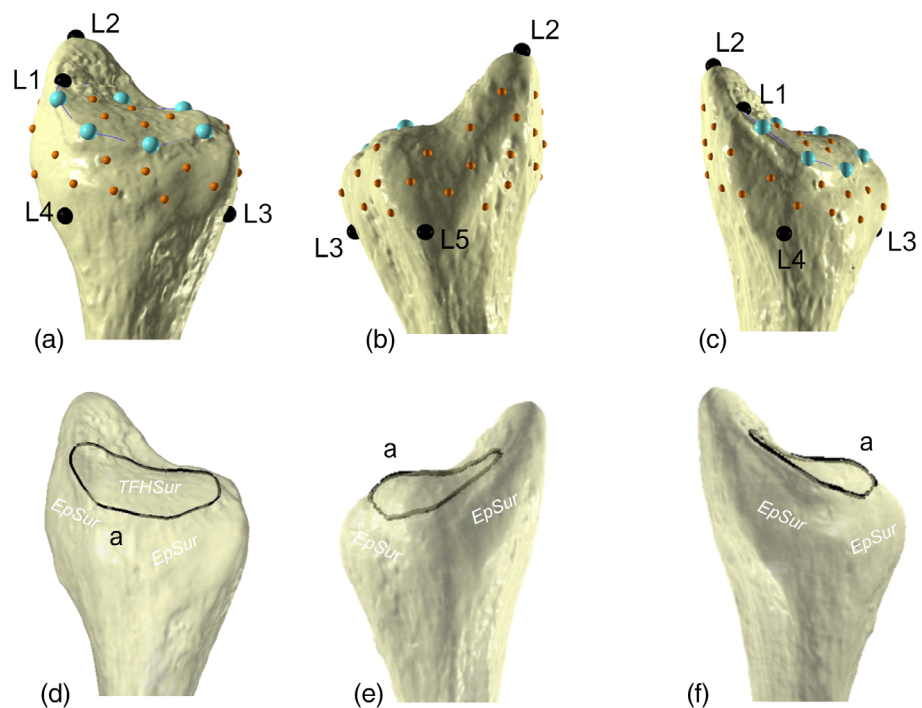
tibia and the facet on the head of the fibula (Sarma et al., 2015). An articular capsule covers the joint, attaching just beyond the articular surfaces of the tibia and the fibula. This capsule is further reinforced by the thick anterior (APTFL) and thinner posterior (PPTFL) proximal tibiofibular ligaments, which also insert through a variable number of bundles into the fibular head anterolaterally and posteriorly (Anavian et al., 2018; Scarciolla et al., 2021). The APTFL inserts into an anterior protrusion in which the anterior border culminates, separating the medial from the lateral surface (White et al., 2011). Immediately lateral to this anterior protrusion and below the attachment of BT and FCL, the proximal origin to m. *peroneus longus* (PL), which acts to evert and plantarflex the ankle is found (Sammarco & Mangone, 2000). Posteriorly, the PPTFL also inserts into a posterior protrusion that superiorly delineates the horse-shoe-shaped attachment area of the m. *soleus*. The anteromedial surface of the fibular head hosts the proximal insertion of the m. *extensor digitorum longus* (EDL; White et al., 2011).

Several studies have classified the PTFJ based on the shape and orientation of the joint surface, and significant variability has been reported (Barnett & Napier, 1952; Eichenblat & Nathan, 1983; Martin & Saller, 1959; Ogden, 1974a, 1974b). In general, the PTFJ ranges from a horizontal, planar articular surface, considered more mobile (i.e., in terms of the fibula), to more oblique articular surfaces, at varying angles with the longitudinal axis of the fibula and with different outlines and depths, which are considered less mobile.

The PTFJ is primarily involved in the dissipation of torsional stresses applied at the ankle joint (Ogden, 1974a, 1974b) while also contributing to the dissipation of lateral tibial bending moments and tensile forces, rather than compressive weight bearing (Ogden, 1974a, 1974b). Indeed, Evans and Bang (1966) found that proximal fibulae were stronger (ultimate tensile and single shearing strength), stiffer

(modulus of elasticity), and had a greater tensile strain (% elongation) in comparisons to femurs (see also Preuschoft, 1971). The fibula contributes to the dissipation of tensile forces via the interosseous membrane and at the PTFJ, which rotates externally when the ankle is in dorsiflexed position (Andersen, 1985; Bozkurt et al., 2003).

Lambert (1971), on the other hand, suggested that the fibula has an additional weight-bearing function, with approximately one-sixth of the static load applied at the ankle transmitted to the PTFJ, in agreement with other studies that found different degrees of fibular load sharing (8%–19%) at varying ankle eversion/inversion angles (Funk et al., 2007). In addition, Lambert (1971) suggested that the force transmitted to the PTFJ was generated by the fibula-talar articulation and facilitated by the inferior tibiofibular ligaments and the interosseous membrane. Similarly, under axial loading, the lateral malleolus migrates distally and laterally to the tibia (Wang et al., 1996).

The PTFJ is also involved in the anteroposterior shifting of approximately 1 cm in both directions according to flexion/extension movements at the knee, moving anteriorly when the knee is in a flexed position and posteriorly when the knee is extended (Ogden, 1974a, 1974b).

1.2 | The proximal fibula in human and nonhuman great apes

The fibular head of great apes does not possess a styloid process; therefore, the fibula articulates directly below the tibial lateral condyle. The appearance of the PTFJ surface is well-defined in great apes and contributes to a superiorly flat fibular head (Martin & Saller, 1959). On the other hand, the human PTFJ articulates against the

4 | WILEY—AMERICAN JOURNAL OF BIOLOGICAL ANTHROPOLOGY
The Official Journal of the American Association of Biological Anthropologists

PIETROBELLI ET AL.

lateral side of the lateral tibial condyle and has a greatly variable shape (Barnett & Napier, 1952; Eichenblat & Nathan, 1983; Ogden, 1974a, 1974b). The fibular neck is more anteroposteriorly slender in humans than the rest of the fibular shaft. In contrast, in great apes, the robusticity of the neck is similar to the rest of the shaft (Susman & Stern, 1982). In humans and African apes, the FCL has a cord-like form, stabilizes the knee laterally, and inserts distally to the anterolateral protrusion of the fibular head (Aiello & Dean, 1990). This anterolateral protrusion is also the attachment area of the distal insertion of the BT. This insertion site is shared among all hominoids, where in African apes, the BT also attaches distally onto the lateral condyle and tuberosity of the tibia, and in Asian apes onto the capsule of the knee joint and variably onto the FCL and the lateral epicondyle of the femur. The two heads of the m. *biceps femoris* are fused at their distal insertion in chimpanzees and modern humans but not in *Pongo* and *Gorilla* (Ferrero et al., 2012). Kaseda et al. (2008) describe the unique morphology of the femoral part of the m. *biceps femoris* in orangutans and suggests it is an adaptation to arboreal behavior due to similarities with Old World monkeys.

In humans, the characteristic shape of the fibular head is determined by the prominence of the styloid process, which culminate both the anterolateral and posterior protuberances and offer attachment to the BT and the PPTFL, respectively (Song et al., 2018, 2020). The apex of the styloid process in humans consists of the attachment site for the PFT, one of the critical structures forming the popliteus complex (LaPrade & Bollom, 2001; Zeng et al., 2011). The primary function of the PFL is to resist the posterior dislocation of the lateral condyle of the tibia (Pasque et al., 2003). Kaplan (1957) reports that the connection between the fibular head and the popliteus complex through the PFL is also found in chimpanzees. However, this configuration is rarely reported, probably due to a lack of precise terminology in evaluating the popliteus complex, which is often described without distinguishing the fibular component of its tendon (PFL). In all hominoids, the m. *popliteus* originates from the lateral meniscus. It is reported that in orangutans, this muscle may have two heads as its origin, one of which is located on the fibular head (Ferrero et al., 2012). In modern humans, the muscle flexes and laterally rotates the femur with a fixed tibia or medially rotates the tibia with the fixed femur, "unlocking" the fully extended knee as flexion begins (Aiello & Dean, 1990). In apes, the muscle is a lateral stabilizer of the knee joint (Aiello & Dean, 1990).

Immediately distal to the attachment of BT and FCL, the anterolateral aspect of the fibular head hosts the proximal insertion of the PL in all hominoids, which extends to the lateral aspect of the proximal fibula shaft in all taxa but *Pan* (Ferrero et al., 2012). In humans, the PL, together with the m. *peroneus brevis*, is active during the second half of the stance phase when the weight is transferred to the anteromedial portion of the foot (Aiello & Dean, 1990; Reeser et al., 1983; Stern & Susman, 1983). In addition, Bavdek et al. (2018) showed that the electromyographic activities of peroneal muscles increased when humans walked on a medially inclined ramp, therefore everting the inverted foot (Marchi et al., 2022). Peroneal muscles are recruited in chimpanzees mainly during the support phase of locomotion on either vertical or horizontal trunks when everting the foot

(Stern & Susman, 1983) and regulate the transfer of weight on the medial part of the inverted foot during climbing in great apes (Marchi et al., 2022).

In all hominoids, the m. *soleus* inserts proximally on the posterior aspect of the head of the fibula, immediately distal to the posterior projection that serves as the attachment site for the PPTFL. In modern humans, the proximal insertion site is horseshoe-shaped, and a second proximal insertion site forms a bony ridge on the medial surface of the tibia. In great apes, on the other hand, the proximal insertion of the m. *soleus* is usually confined to the fibular head and occasionally can have a proximal accessory insertion on the tibia (Aiello & Dean, 1990; Prejzner-Morawska & Urbanowicz, 1981). The elongation of the m. *soleus* insertion shape was previously suggested as determining the fibular head shape in humans, which culminates in the styloid process, versus that in apes, which possess a flat head (Martin & Saller, 1959). The m. *soleus* of *Gorilla* and *Pan* is bulkier than that of the Asian apes (Ferrero et al., 2012). In humans, the whole m. *triceps surae* is twice as heavy as in *Pan*, reflecting its involvement in lifting the whole-body weight in bipedal locomotion (Aiello & Dean, 1990). A medial expansion of m. *soleus* seen in apes may be functionally related to an arboreal lifestyle with significant amounts of vertical climbing (Hanna & Schmitt, 2011), with medial fibers more active than lateral fibers in foot inversion (O'Connell, 1958).

The anteromedial surface of the fibular head provides attachment for the m. *extensor digitorum longus*, an extensor of the II-IV toes (Aiello & Dean, 1990), in all hominoids. In *Gorilla*, there is also an origin from the anterior surface of the shaft of the fibula (Ferrero et al., 2012).

1.3 | Aim of the work

In this study, we provide a detailed comparative assessment of shape variation of the proximal fibula in extant humans and great apes using 3D-GM to detail the variation of proximal fibular shape in each taxon and investigate a possible link with locomotor and positional behaviors. The 3D-GM approach has been applied to human and nonhuman primate bones by many recent studies to address functional questions providing valuable information for the assessment of shape variation of postcranial skeletal elements and functional interpretation of fossil material (Almécija et al., 2013; Frelat et al., 2017; Harcourt-Smith et al., 2008; Harmon, 2006, 2007, 2009; Marchi et al., 2022; Sorrentino, Carlson, et al., 2020; Sorrentino, Stephens, et al., 2020; Turley et al., 2011).

Based on previous studies outlined above, we expect that the shape of the fibula in extant hominids will significantly differ between humans and great apes because the different locomotor and postural repertoires entail different loading regimens applied at the knee in flexion (Aiello & Dean, 1990; Isler, 2005; Scott et al., 2007) and at the ankle in dorsiflexion and eversion (Ogden, 1974a, 1974b).

In particular, we expect to find the following:

1. A more horizontal proximal tibiofibular articular surface in great apes than in humans, previously linked to higher mobility of the knee (Frelat et al., 2017; Sylvester, 2013; Sylvester & Pfisterer,

PIETROBELLI ET AL.

AMERICAN JOURNAL OF
BIOLOGICAL ANTHROPOLOGY
The Official Journal of the American Association of Biological Anthropologists

WILEY 5

2012; Tardieu, 1999) and ankle (DeSilva, 2009; Latimer et al., 1987; Barnett & Napier, 1953; Stern & Susman, 1983).

2. A superiorly elongated fibular head (i.e., presence of the styloid process) in humans in comparison to a flat fibular head in great apes, contributing to the knee "unlocking mechanism" in bipedal standing in the former group (Aiello & Dean, 1990);

3. An anterolateral expansion of the fibular head suggesting more powerful hamstrings and peroneal muscles in great apes than in humans, linked to the stabilization of the inverted foot during vertical climbing and walking/clambering (Stern & Susman, 1983);

4. A proximo-distally elongated insertion of the m. *soleus* in humans due to its greater mass relative to the whole m. *triceps surae*, with a medially expanded insertion area in apes, as it is considered an indicator of a greater degree of arborealism (Hanna & Schmitt, 2011).

Finally, a further goal of this study is to lay the ground for further investigations of the proximal fibula of extinct hominins, as this element is preserved in the fossil record (e.g., *Australopithecus sediba*, DeSilva et al., 2013; StW 573 "Little Foot," Heaton et al., 2019; *Homo floresiensis*, Jungers et al., 2009; *Homo neanderthalensis*, Trinkaus, 1983) but rarely quantitatively compared or analyzed.

2 | MATERIALS AND METHODS

2.1 | The sample

The analyzed sample includes a total of 94 fibulae belonging to 37 *H. sapiens*, 15 Gorilla (*Gorilla gorilla* = 12; *Gorilla beringei* = 3), 17 *Pongo* (*Pongo abelii* = 8; *Pongo pygmaeus* = 9), and 25 *Pan* (*Pan troglodytes* = 24; *Pan paniscus* = 1; Table 1). All fibulae belong to adult individuals with fully fused epiphyseal lines according to the visual estimation criteria (Belcastro et al., 2019) and without signs of pathology in the skeleton. The fibulae were selected based on their general good state of preservation. For each individual, the left fibula was used. When the left fibula was unavailable, the right one was digitally mirrored.

Three-dimensional surface meshes of the fibula belonging to the University of Bologna (UNIBO) institution were digitized through computed tomography (CT), utilizing a Revolution Discovery CT dual energy at Istituto Ortopedico Rizzoli (Bologna, Italy; slice thickness and increment at 0.625 mm, voltage 100 kV, X-ray tube current 360 mA, reconstruction at 40 keV with "Detail" filter, voxel size ranging from 0.39 to 0.507 x 0.625 mm). The reconstructed DICOM (16-bit gray-scale, signed) images were then processed with Avizo 9.2

TABLE 1 Sample composition

Taxon	n	Institution	Sex		Side		
			Male	Female	Unknown	Right	Left
Homo sapiens	37	UNIBO	17	20	-	-	37
Pan troglodytes	24	AMNH, NMNH, UZH, SZCM, KUPRI, UNIBO	15	7	2	13	11
Pan paniscus	1	AMNH	-	1	-	-	1
Gorilla gorilla	12	AMNH, UZH, SZCM, KUPRI	8	4	-	7	5
Gorilla beringei	3	AMNH, NMNH	2	1	-	2	1
Pongo pygmaeus	9	AMNH, NMNH, UZH, SZCM,	3	6	-	7	2
Pongo abelii	8	NMNH, UZH, SZCM, KUPRI	7	1	-	5	3

Abbreviations: AMNH, American Museum of Natural History (via www.morphosource.org); KUPRI, Primate Research Institute's Digital Morphology database; NMNH, National Museum of Natural History (via www.morphosource.org); SZCM, State Zoological Collection in Munich; UNIBO, Human Identified Skeletal Collection of Bologna; UZH, University of Zurich.

TABLE 2 Fibular landmarks and semilandmarks identification, definition, and number

Landmarks	Definition	
L1	Most proximal point of proximal tibiofibular articular facet	
L2	Most proximal point on styloid process of fibular head in medial view	
L3	Most anteroproximal point on anterior border in medial view (proximal to fibular neck)	
L4	Most posters-proximal point on posteromedial border in medial view (proximal to fibular neck)	
L5	Most posters-proximal point on posterior border in lateral view (proximal to fibular neck)	
Curves	Definition	Number of semi-landmarks
a	Outline of *proximal tibiofibular articular facet*	6
Surfaces	Definition	Number of semi-landmarks
TFHSur	Proximal *tibiofibular articular surface*	5
Sur	Surface of *proximal epiphysis*	32

TABLE 3 Summary of the relevant morphological features observed in the four genera analyzed (*Homo*, *Pan*, *Gorilla* and *Pongo*)

Features	Genera			
	Gorilla	*Pan*	*Pongo*	*Homo sapiens*
Overall fibular head shape	Squared shape in medial view (anteroposteriorly expanded), with inferiorly projecting, pointed fibular collateral ligament attachment.	Rectangular shape in medial view (anteroposteriorly expanded) with inferiorly projecting, pointed fibular collateral ligament attachments.	Sub-circular shape in medial view (regular proportions anteroposteriorly and mediolaterally) with projecting, pointed collateral ligament attachments.	Squared shape in medial view (regular proportions anteroposteriorly and mediolaterally) with a superiorly raised styloid process (orange arrow) and well-rounded but diminished tibiofibular collateral ligament attachments, located more superiorly.
Anterior border	Well-marked, straight and raised, with an acute border facing anteromedially	Marked and raised with an acute border curving anteriorly at most proximal point	Evident and straight, facing anteromedially, with a more convex border.	Defined and straight, with a convex border facing medially
Medial surface	Moderately concave below the articular border. Some degree of anterior expansion is present, mostly related to the inferior expansion of the m. biceps femoris (see below).	Flattened, anteroposteriorly expanded	Marked concavity below the articular border that prolongs to the neck level. The black arrow indicates the anterolateral expansion at the m. peroneus longus attachment area (see below).	Flattened
Fibular neck shape	Oval dimensions (anteroposteriorly expanded)	Oval dimensions (anteroposteriorly expanded)	Circular dimensions (regular proportions anteroposteriorly and mediolaterally)	Oval dimensions (anteroposteriorly expanded)
Tibiofibular articular surface	Slightly anteroposteriorly oblique, but approximately horizontal mediolaterally	Horizontal anteroposteriorly and mediolaterally	Slightly anteroposteriorly oblique, but approximately horizontal mediolaterally	Either markedly oblique mediolaterally and slightly anteroposteriorly oblique
Mm. peroneus longus/ biceps femoris attachment areas	The attachment area of the biceps femoris tendon is defined and inferiorly expanded (orange arrow), showing a depressed area (imprint, black circle) corresponding to the lateral collateral ligament, facing laterally, while the attachment area of m. peroneus longus, immediately below (black lines) is concave, more anterolaterally facing, expanded laterally in comparison to chimpanzees but not quite as orangutans.	The attachment area of the biceps femoris tendon is defined and inferiorly expanded (orange arrow), showing a slightly depressed area (imprint, black circle) corresponding to the lateral collateral ligament, facing laterally, while the attachment area of m. peroneus longus, immediately below (black lines) is more anterolaterally facing but slightly concave.	The attachment area of the biceps femoris is laterally expanded (orange arrow), showing narrow, deep depression (imprint, black circle), corresponding to the lateral collateral ligament facing laterally. The attachment area of m. peroneus longus, immediately below (black lines) is concave and markedly anterolaterally protruding. This is also evident in medial view (see above), where this area is expanded, quite hollow, and inferiorly elongated	The attachment area of the biceps femoris is posteriorly expanded towards the styloid process and rounded anterolaterally (orange arrow). Superiorly, it is present an attenuated depression (imprint, black circle) corresponding to the lateral collateral ligament, facing superiorly. The attachment area of m. peroneus longus (black lines) is narrow and facing anteriorly, with medial expansion and rather flat.
m. soleus attachment area	The area on the insertion is well defined and has a wide horseshoe shape with posteromedial expansion. It is delimited superiorly by a robust posterior projection for	The area on the insertion is well defined and had has a wide horseshoe shape with posteromedial expansion. It is delimited superiorly by a robust posterior projection for	The area on the insertion is defined and has a narrow sub-circular shape, medially expanded but less inferiorly elongated. Superiorly, the posterior projection for the	The area on the insertion has reduced anteroposterior dimensions but is appreciable as a deep horse- shoe groove, facing posteriorly. It is

PIETROBELLI ET AL.

AMERICAN JOURNAL OF
BIOLOGICAL ANTHROPOLOGY
The Official Journal of the American Association of Biological Anthropologists

WILEY 7

TABLE 3 (Continued)

Features	Genera			
	Gorilla	Pan	Pongo	Homo sapiens
	the posterior proximal tibiofibular ligament	the posterior proximal tibiofibular ligament	posterior proximal tibiofibular ligament is well rounded and not inferiorly elongated.	elongated proximo-distally. It is delimited superiorly by a robust posterior projection for the posterior proximal tibiofibular ligament that culminates superiorly into the styloid process

(Thermo Fisher Scientific) for image segmentation with a modified version of the half-maximum height (HMH) protocol (Coleman & Colbert, 2007; Spoor et al., 1993). Lastly, an isosurface was generated for each segmentation.

Three-dimensional surface meshes of ape fibulae belonging to the State Zoological Collection in Munich (SZCM), Germany, and the University of Zurich (UZH), Switzerland, were obtained using medical CT scanning. The SCM specimens were collected at the Munich Institute for Radiology Ludwig Maximilian University (Munich, Germany) on a GE Discovery CT750 HD medical CT scanner (slice thickness 0.625 mm, slice increment 0.3 mm, voltage 120 kV, X-ray tube current 99 mA, reconstructing algorithm bone, pixel size 460 μm). The UZH specimens were collected at the University Hospital of Zurich (Zurich, Switzerland) on a Siemens Somaton Definition Flash (slice thickness 0.6 mm, slice increment 0.3 mm, voltage 120 kV, current 19 mA, reconstructing algorithm bone, pixel size 600 μm). Similar to the UNIBO sample, the SZCM and UZH samples were segmented utilizing the HMH segmentation protocol detailed previously. All UNIBO, UZH, and SZCM samples consisted of dry bone specimens.

Selected fibulae belonging to the Division of Mammals, National Museum of Natural History, Smithsonian Institution, and the Mammal Collections at the American Museum of Natural History were obtained via MorphoSource (https://www.morphosource.org/). The specimens include dry bone samples, and the digital models were obtained either by laser scanning or CT scanning. MorphoSource Media IDs and Institution collection numbers of these specimens are displayed in the Appendix S1.

Other ape specimens used in this study were obtained via Digital Morphology (KUPRI) from the Primate Research Institute's (PRI) collection of CT scans. For these specimens, scan resolution (X, Y) ranged from 0.133 to 0.761 mm, with a slice thickness (Z) of 1–2 mm. The specimens included dry bones, fresh cadavers, and other samples with frozen or immersed soft tissue.
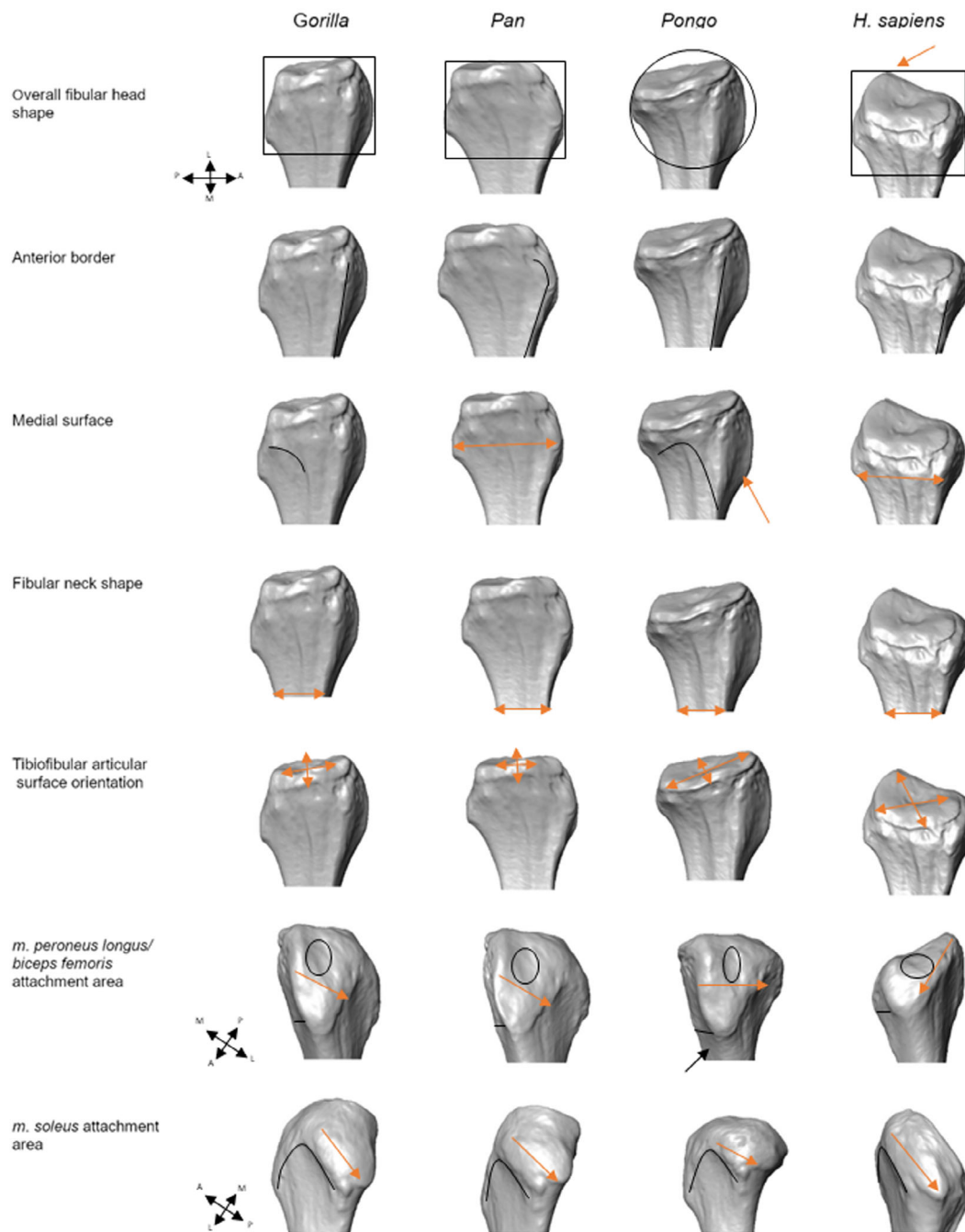
2.2 | 3D geometric morphometric analysis

A 3D template configuration (Figure 1, Table 2) of 16 fixed landmarks, 25 curve semilandmarks, and 101 surface semilandmarks captured the proximal extremity of the fibula. The template was created in Viewbox 4 to cover major muscle, ligament, and tendon attachment sites and articular surfaces on the proximal fibula (Figure 1, Table 2). Next, Viewbox software was utilized to apply the template configuration to the sample of proximal fibulae (targets), with semilandmarks sliding on curves and surfaces to minimize thin-plate spline (TPS) bending energy between the targets and the template (Slice, 2006). Following that, semilandmarks can be considered geometrically homologous among specimens (Gunz et al., 2006; Gunz & Mitteroecker, 2013). The template repeatability (i.e., high intra-observer agreement) and reproducibility with different scanning devices were tested in a previous study (Pietrobelli et al., 2022). Landmark and semilandmark raw coordinates used are available in the Appendix S2 and S3. After importing raw coordinates in R (version 4.0.3; R Core Team, 2020), a further sliding step was performed against recursive updates of the Procrustes consensus (R package "geomorph"; Adams et al., 2018), while a Procrustes superimposition was computed. This procedure allowed the conversion of raw coordinates into standardized, scaled, centered, and oriented shape coordinates (i.e., Procrustes coordinates) via generalized procrustes analysis (GPA; Rohlf & Slice, 1990; Slice, 2006). Outliers from Procrustes consensus were detected utilizing the function plotOutliers() provided in this package. The centroid size (CS) was also calculated and used as a proxy for the size of the proximal end of the fibula (Slice, 2006).

Procrustes coordinates were then subjected to a principal component analysis (PCA) to explore shape variations among the different genera (Schlager, 2017). Finally, principal component (PC) scores were evaluated and compared among genera using a one-way ANOVA, with subsequent post hoc pairwise comparisons, and visualized as violin plots.

Visualization of shape changes along the principal axes and means based on genera were obtained by TPS deformation (Bookstein, 1991) of the Procrustes grand mean shape surface utilizing the R package "Morpho" v. 2.8 (Schlager, 2017). In addition, visualizations of the mean shape distances among mean configuration according to genera and Procrustes consensus were computed utilizing the function localmeshdiff() from the package "Arothron" v. 2.0.3 (Melchionna et al., 2020; Profico et al., 2021).

Procrustes ANOVA was used to test shape differences among genera, utilizing Procrustes distances among specimens and using a residual randomization procedure (RRPP = T, iterations = 1000), with the R package "geomorph" v. 3.3.2 (Adams et al., 2018). Differences in size among genera were evaluated using ANOVA and subsequent post hoc tests and visualized in relative box plots. Procrustes distance distribution

8 WILEY—**AMERICAN JOURNAL OF BIOLOGICAL ANTHROPOLOGY** The Official Journal of the American Association of Biological Anthropologists

PIETROBELLI ET AL.

FIGURE 2 Schematic representation of the major morphological differences in the proximal fibula between *Gorilla*, *Pan*, *Pongo* and *Homo sapiens* (bones from left side are shown). Fibular shapes shown refer to extreme configurations obtained for each genus along the first two principal components. The first five rows show fibulae in medial view, the last two show fibulae in antero-lateral and postero-lateral view, respectively. At the top row, shapes indicate the overall morphology of the fibular head. At the second row, curved lines indicate the outline of the anterior border. The third row, arrows represent flat medial surface, while curves represent the concavity of medial surface. The *Pongo* specimen on the third row also shows an orange arrow indicating the concavity relative to the PL (see below, line fifth). Arrow in the fourth row shows the thickness of the fibular neck, with a slender circular shape for *Pongo* and expanded for the rest. At fifth row, orange arrows show the orientation of PTFJ. At sixth row, black empty ellipses indicate the FCL insertion, orange arrows show the projection of the PL/BT area, black lines show the antero-lateral expansion of the PL, and black arrows show the lateral expansion of the PL. At bottom row, black lines show the outline of m. soleus insertion, orange arrows indicate the inferior projection of the area of insertion of PPTL. PTFJ: proximal tibio-fibular joint; PPTFL: anterior proximal tibiofibular ligaments; FCL: fibular collateral ligament; BT: m. biceps femoris tendon attachment; PL = *m. peroneus longus* origin.

PIETROBELLI ET AL.

AMERICAN JOURNAL OF
BIOLOGICAL ANTHROPOLOGY
The Official Journal of the American Association of Biological Anthropologists

WILEY | 9

was also visualized by computing density values of Procrustes distances of each specimen to the Procrustes consensus, separated by genus.

The form-space (i.e., shape plus size) PCA was computed by augmenting the Procrustes shape coordinates of each dataset of Procrustes coordinates by the natural logarithm of CS (lnCS; Klingenberg, 2016). Linear correlation among CS and the PC scores along the first two shape PCs was assessed by a Pearson's correlation test to assess whether the distribution of individuals in the shape space PCA plot was influenced by size. All these analyses were then repeated, excluding the *H. sapiens* sample and considering the great apes' sample only.

3 | RESULTS

A summary of the morphological differences observed among the sampled genera is presented in Table 3 and detailed in Figure 2.

3.1 | All extant hominoid genera

Figure 3 shows the shape space PCA scatterplots of *Pan*, *Gorilla*, *Pongo*, and *H. sapiens* and extreme shape variations along the first three PCs, which account for 63.9% of the total variance (PC1: 47.5%; PC2: 9.3%; PC3: 7.1%).

The plot of PC1 against PC2 (Figure 3) clearly shows the separation along PC1 between *H. sapiens*, plotting towards PC1 positive scores, and great apes, plotting towards PC1 negative scores (Figures 3 and 4). While all great apes taxa show some degree of overlap along PC1, *Pongo* and *Pan* PC scores differ significantly (Table 4). PC1 positive extreme shape, characterizing *H. sapiens*, is driven mainly by a well-marked styloid process, an anteroinferior, posterior superiorly angled PTFJ, and presents a squared head in lateral view, a thicker neck, a flat medial surface, a raised anterior border, a moderately anteriorly facing and well-defined flat area of insertion for PL/BT, and an
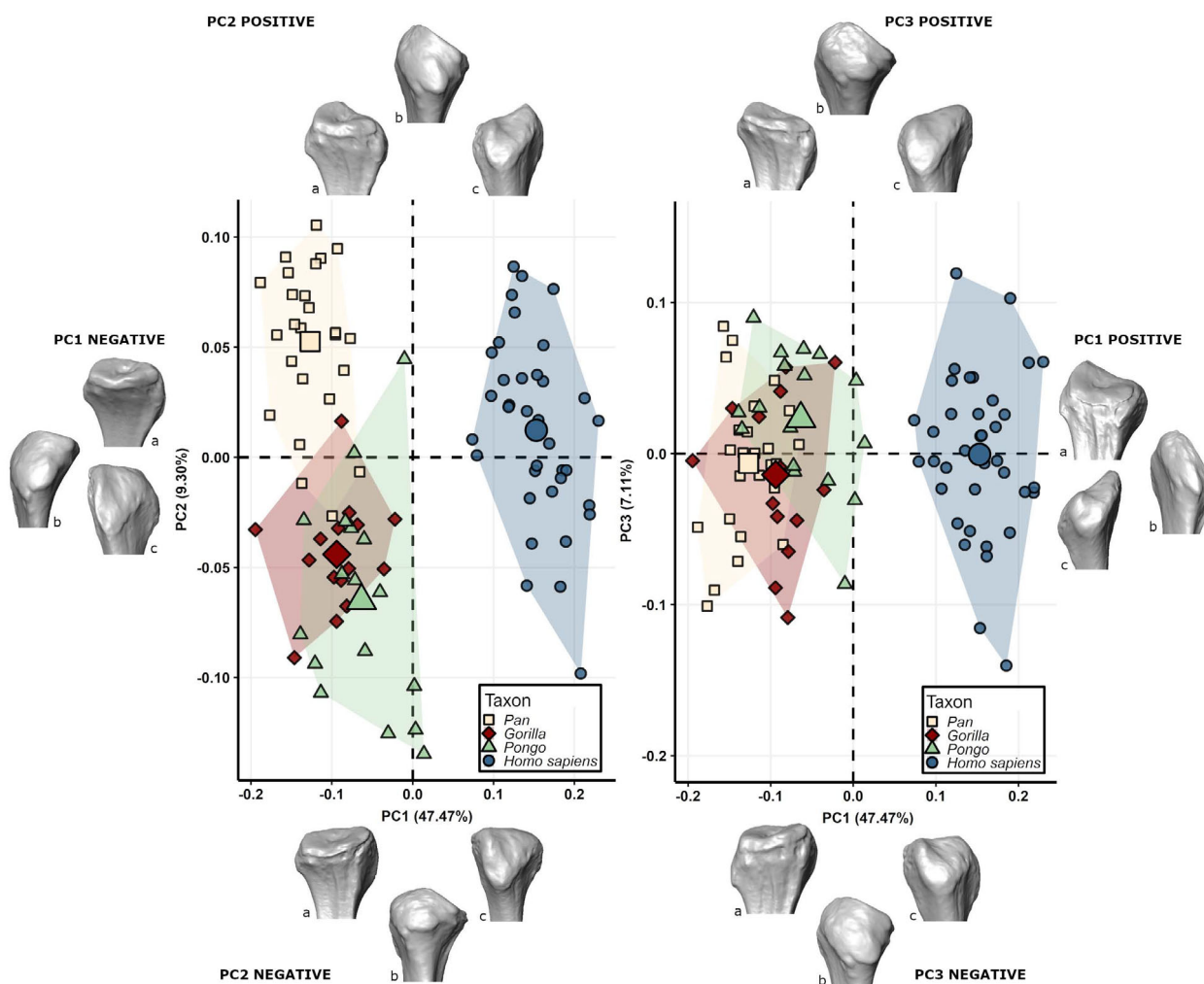
FIGURE 3 Shape space scatterplots of second versus first component (PC2 vs. PC1, on the left) and third versus first principal component (PC3 vs. PC1, on the right, B) of *Pan* (yellow squares), *Gorilla* (red rhombuses), *Pongo* (green triangles) and *Homo sapiens* (blue circles) and relative means, with shape space extreme morphings in medial (a), posterior (b) and antero-lateral (c) views of a left fibula, originally belonging to a *Gorilla* specimen, then morphed according to the extreme shape reconstruction along the principal axes. PC1 extreme positive and negative morphings are displayed on the right and the left, respectively. PC2 extreme positive and negative morphings are displayed at left top and left bottom, respectively, while PC3 extreme positive and negative morphings are displayed at right top and right bottom.

10 | WILEY—AMERICAN JOURNAL OF BIOLOGICAL ANTHROPOLOGY
The Official Journal of the American Association of Biological Anthropologists

PIETROBELLI ET AL.
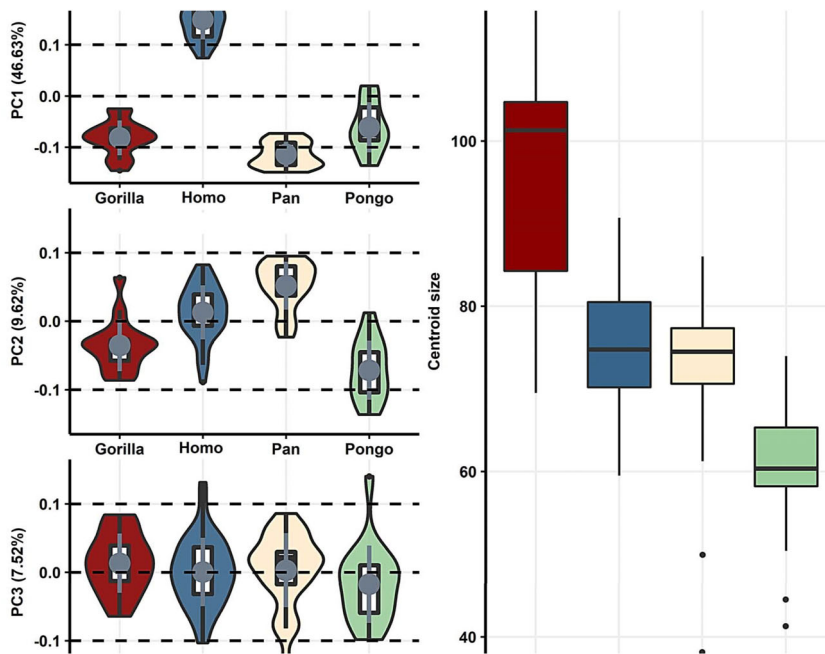
FIGURE 4 On the left, violin plots representing the distribution of principal component (PC) scores along the first three PC of *Pongo*, *Gorilla*, *Pan* and *Homo sapiens*. Gray circles are the medians, black boxes represent the interquartile ranges, whiskers the non-outliers range. On the right, box plots representing centroid size variations of *Pongo*, *Gorilla*, *Pan* and *H. sapiens*. Black lines are the medians, black boxes represent the interquartile ranges, whiskers the non-outliers range and black circles the outliers. Asterisks show ANOVA post hoc significant comparisons of centroid size among groups.

TABLE 4 Pairwise *t*-test on principal components (PC) 1 and PC2 scores *Pan*, *Gorilla*, *Pongo* and *Homo sapiens*. Results in bold are statistically significant. Results above the diagonal represent group comparisons along PC1, while results below the diagonal represent group comparisons along PC2.

PC2	PC1			
	Pan	*Gorilla*	*Pongo*	*H. sapiens*
Pan	-	0.060	**0.000**	**0.000**
Gorilla	**0.000**	-	0.140	**0.000**
Pongo	**0.000**	0.434	-	**0.000**
H. sapiens	**0.001**	**0.000**	**0.000**	-

TABLE 5 Post hoc pairwise comparisons among *Pongo*, *Gorilla*, *Pan* and *Homo sapiens* after Procrustes ANOVA. Results in bold are statistically significant

	Gorilla	*Pongo*	*H. sapiens*
Pan	**0.011**	**0.001**	**0.000**
Gorilla	-	0.136	**0.000**
Pongo		-	**0.000**

diverge from one another regarding Procrustes distances, except for gorillas and orangutans (Table 5, Figure S2).

Mean shapes for each genus are represented in Figure S3 and display a trend already observed with the extreme shapes that distinguish humans from great apes.

Regarding the CS comparisons, *Gorilla* and *Pongo* show the most prominent and undersized proximal ends, respectively (Figure 4), and are significantly different from all other genera. *Homo sapiens* and *Pan* display comparable CS means and distributions. All PC scores along the three first shape PCs do not significantly correlate with CS. A clear separation between *H. sapiens* and great apes is present in the form space PCA along PC2, and Pongo is clearly separated from *Gorilla* along PC1 with *Pan* plotting in between (Figure 5).

3.2 | Apes only

Figure 6 shows the shape space PCA scatterplots for *Pan*, *Gorilla*, and *Pongo* and extreme shape variations along the first three PCs, which account for 49.6% of the total variance (PC1: 23.9%; PC2: 13.6%; PC3: 12.1%). Again, more apparent separation is observed among the great apes when humans are excluded from the analysis.

The plot of PC1 against PC2 (Figure 6) shows that along PC1, *Pan* plots towards negative scores, *Pongo* toward positive scores, and

inferiorly elongated attachment area of the m. *soleus*. PC1 negative extreme shape, characterizing great apes, is mainly driven by a horizontal PTFJ with an absent styloid process, a rectangular head in lateral view, a slender neck, a concave medial surface, an inferiorly elongated PL/BT insertion area which is less expanded laterally in comparison to all other extremes, and a posteromedially expanded m. *soleus* attachment area that is less defined and surmounted by a rounded protrusion posteriorly.

Along PC2, *H. sapiens* overlaps with all great apes. *Pan* clusters with more positive scores within great apes and is significantly different from the other genera (Table 4). *Gorilla* and *Pongo* overlap extensively, with *Pongo* showing greater dispersion. *Pan* shows a rounded head in lateral view, a slender neck, an approximately horizontal PTFJ, a slightly concave medial surface, an inferiorly elongated PL/BT insertion area, and a posteromedially expanded m. *soleus* attachment area that is less defined and surmounted by a rounded protrusion posteriorly. *Pongo* and *Gorilla* show, in comparison, a more rounded fibular head and a more pronounced laterally expanded PL/BT insertion.

All taxa overlap extensively along PC3, with no significant differences (*p* > 0.05) in distribution (Figures 3 and 4). However, all groups

FIGURE 5 Form space principal component analysis scatterplots considering principal component (PC) scores of *Pan* (yellow squares), *Gorilla* (red diamonds), *Pongo* (green triangles) and *Homo sapiens* (blue circles) and relative group means along the first two PCs.
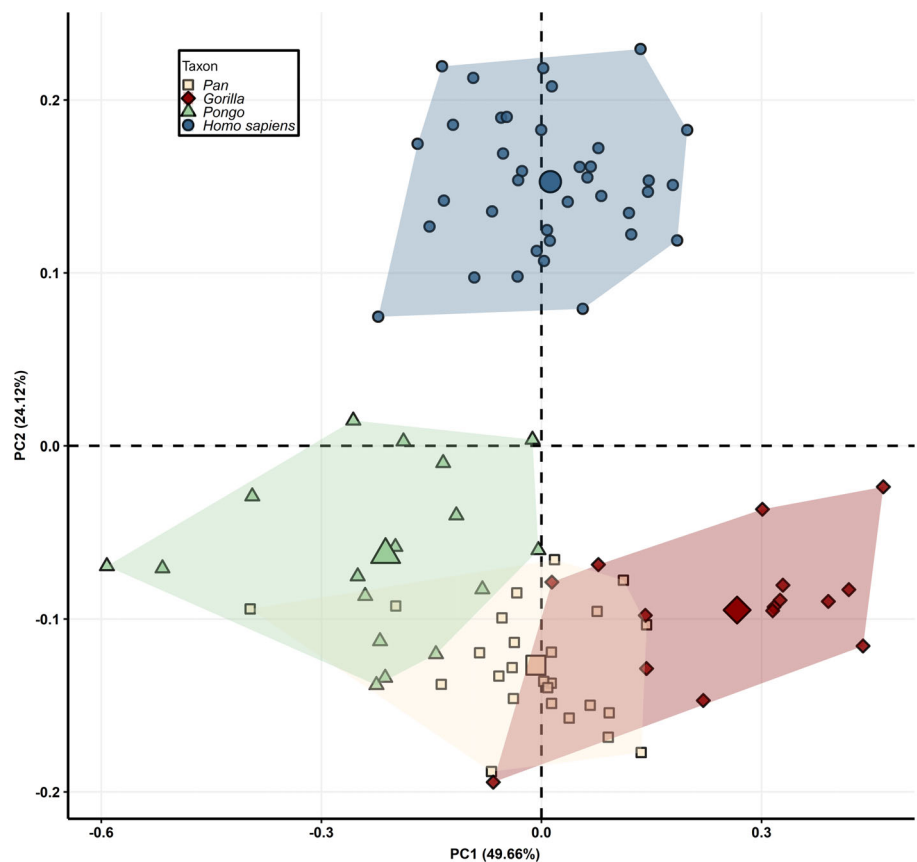
Gorillas is in between, slightly overlapping with both *Pan* and *Pongo* towards positive scores. Along PC1, all great apes differ significantly from one another (Figure 7 and Table 6).

Pongo (PC1 positive) shows a slightly circular fibular head in lateral view, a narrower neck, with an anterosuperior posterior-inferiorly angled PTFJ oblique PTFJ, a concave medial surface right distal the PTFJ border, a defined anterior border, a marked laterally protruding insertion areas of PL/BT, a narrow, deep attachment for the FCL, and a less inferiorly elongated, sub-circular m. *soleus* attachment area, superiorly delineated by a well-rounded protrusion for the PPTFL.

Pan (PC1 negative) displays a rectangular fibular head in lateral view and a slender neck, a horizontal PTFJ, a flat medial surface, and a well-delineated area for PL/BT, which is inferiorly expanded but less laterally projected, with a superior impression for FCL and a deep, oval attachment of m. *soleus*, with posteromedial expansion.

All taxa overlap extensively along PC2 or PC3 (Figures 6 and 7). The only significant difference is between *Pongo* and *Gorilla* along PC2 (Table 6). All groups differ in the Procrustes distance (Table 7, Figure S4). Shape variation along PC2 is similar to that observed along PC1. It primarily refers to a more lateral projection of PL/BT (PC2 positive) and a slightly anteroposteriorly oblique PTFJ towards positive scores, with a posteromedial expansion for the m. *soleus* attachment, less inferiorly elongated in *Pongo* (PC2 negative). PC3 mainly refers to an inferiorly elongated and narrow (PC3 positive) compared with an anteroposteriorly expanded and shorter (PC3 negative scores) fibular head.
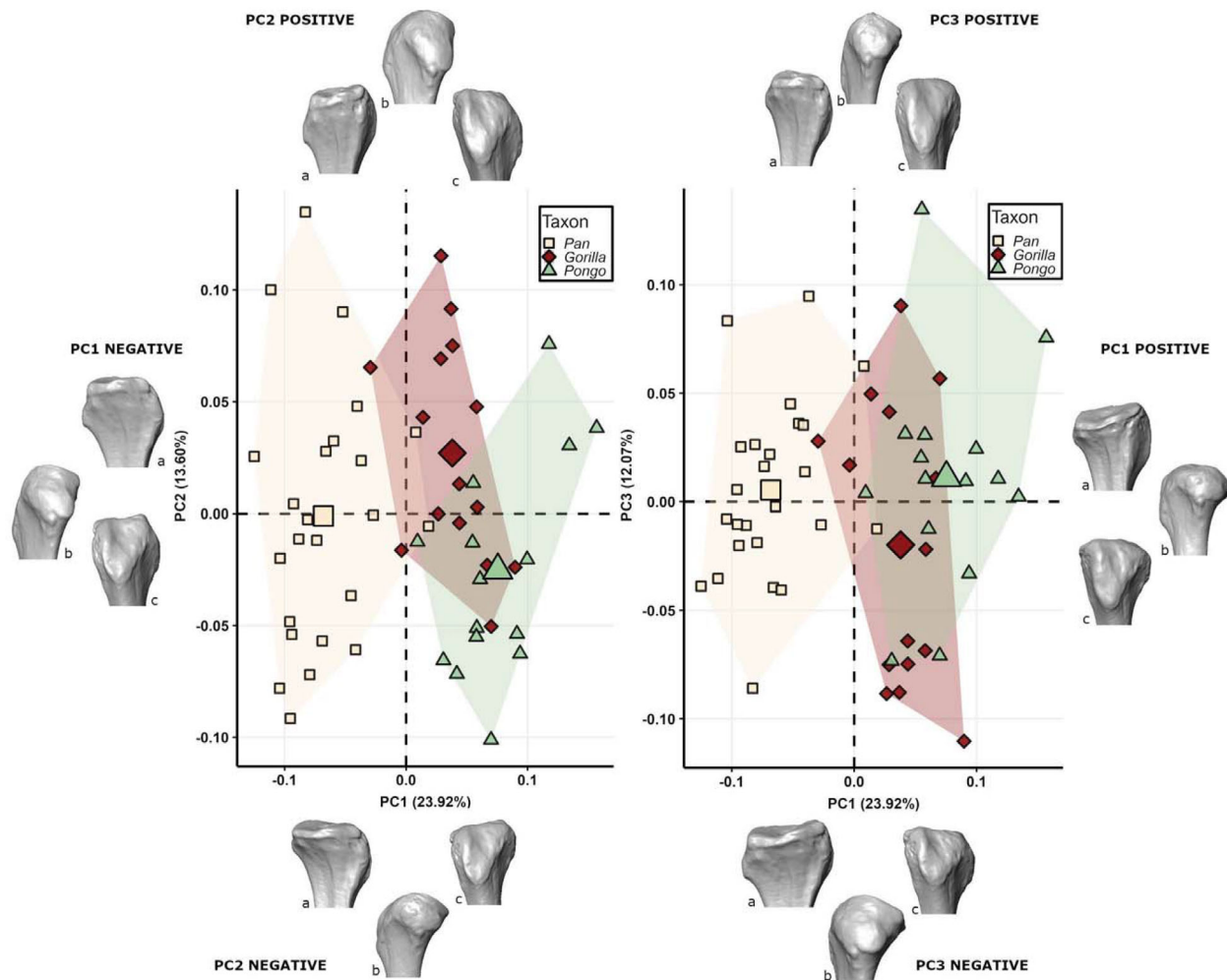
Mean shapes for each genus of the great apes display similar morphologies to those already observed in extreme shape reconstructions along PCs (Figure S5).

Concerning CS comparisons and form space variations, *Gorilla* and *Pongo* show the most significant and minor proximal epiphyseal size, respectively (Figures 7 and 8). The form space bivariate plot of PC1 against PC2 shows segregation among the three genera. None of the PC scores along the three first PCs significantly correlates to CS.

4 | DISCUSSION

In this study, we have provided a thorough morphometric description of the proximal fibula in extant hominids by the 3D-GM approach. In addition, we hypothesized significantly different shape changes among extant significant ape taxa and humans in response to these groups' different ankle and knee loading regimens. Our results are consistent with our hypotheses and highlight variation comparable to previous evaluations of distal fibular morphology among extant hominids (Marchi, 2015b; Marchi et al., 2022; Stern & Susman, 1983), further highlighting the functional role of the fibula and its potential in inferring mobility patterns in early hominins.

In particular, in humans, we expected to find a more angled proximal tibiofibular joint (PTFJ), the presence of the styloid process, reduced anterolateral and inferior expansion of the hamstrings and peroneal muscles insertion areas on the fibular head as well as a deep

12 | WILEY | AMERICAN JOURNAL OF BIOLOGICAL ANTHROPOLOGY
The Official Journal of the American Association of Biological Anthropologists

PIETROBELLI ET AL.

FIGURE 6 Shape space scatterplots of second versus first component (PC2 vs. PC1, on the left) and third versus first principal component (PC3 vs. PC1, on the right) of *Pan* (yellow squares), *Gorilla* (red rhombuses) and *Pongo* (green triangles) and relative means, with shape space extreme morphings in medial (a), posterior (b) and antero-lateral (c) views of a left fibula, originally belonging to a Gorilla specimen, then morphed according to the extreme shape reconstruction along the principal axes. PC1 extreme positive and negative morphings are displayed on the right and the left, respectively. PC2 extreme positive and negative morphings are displayed at left top and left bottom, respectively, while PC3 extreme positive and negative morphings are displayed at right top and right bottom.

insertion of the m. *soleus*. In contrast, great apes were expected to possess a more horizontal PTFJ, a superiorly flat fibular head, an antero-lateral and inferior expansion of the hamstring and peroneal muscles insertion areas onto the fibular head, and a defined but shallower, more medially expanded m. *soleus* insertion. The presence of these shape changes in our sample is in agreement with the expected higher mobility of the ankle (Barnett & Napier, 1953; DeSilva, 2009; Latimer et al., 1987; Stern & Susman, 1983) and knee joints (Frelat et al., 2017; Sylvester, 2013; Sylvester & Pfisterer, 2012; Tardieu, 1999) in great apes and with the unique knee "unlocking mechanism" present in modern humans when initiating knee flexion (Aiello & Dean, 1990). Moreover, the observed anterolateral, inferior and medial expansion of the hamstring and peroneal tendon insertions in great apes agrees with the need for stabilization of an inverted foot during vertical climbing and walking/clambering (Stern & Susman, 1983) and with a greater degree of arborealism (Hanna & Schmitt, 2011). On the other

hand, the observed deeper insertion of the m. *soleus* in modern humans may indicate its relatively greater muscle mass than the whole *triceps surae*, necessary for bipedal walking and running (Hanna & Schmitt, 2011).

4.1 | Differences between humans and great apes

The results of our morphometric comparison between the proximal fibula of modern humans and extant great apes provide further support to the functional role of the fibula in humans, highlighting a suite of morphological features that appear correlated with bipedalism (Harcourt-Smith, 2015). For example, the more angled PTFJ (Figures 2 and 3) in humans may indicate a less mobile articulation (Eichenblat & Nathan, 1983; Ogden, 1974a, 1974b; Sarma et al., 2015). Indeed, in the past, the angle of the PTFJ was associated with a reduced

FIGURE 7 On the left, violin plots representing the distribution of principal component (PC) scores along the first three PCs of *Pongo*, *Gorilla* and *Pan*. Gray circles are the medians, black boxes represent the interquartile ranges, whiskers the non-outliers range. On the right, box plots representing centroid size variations of *Pongo*, *Gorilla* and *Pan*. Black lines are the medians, black boxes represent the interquartile ranges, whiskers the non-outliers range and black circles the outliers. Asterisks show ANOVA post hoc significant comparisons of centroid size according to groups.
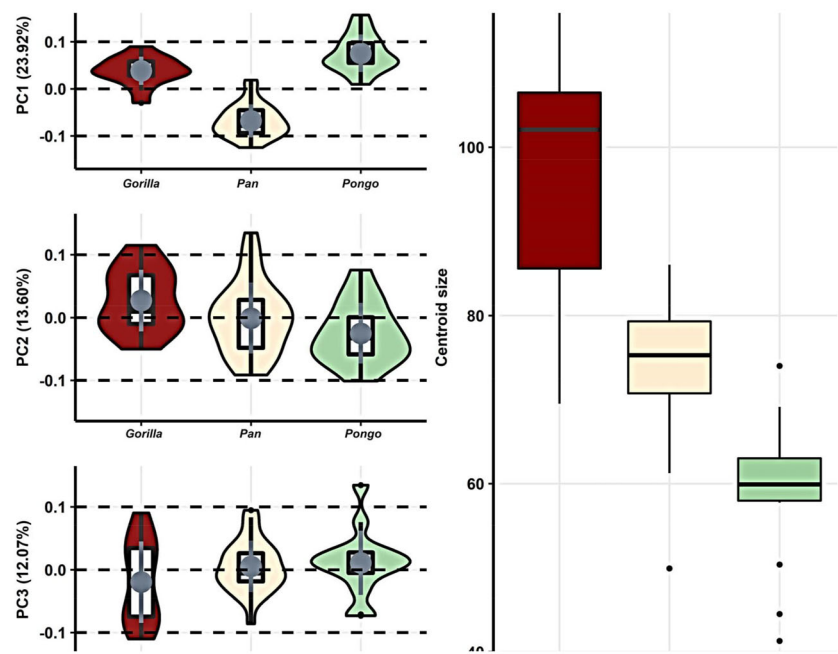
TABLE 6 Pairwise *t-test* on principal components (PC) 1 and PC2 scores of *Pan*, *Gorilla* and *Pongo*. Results in bold are statistically significant. Results above the diagonal represent comparisons along PC1, while result below the diagonal represent comparisons along PC2

	PC1		
PC2	*Pan*	*Gorilla*	*Pongo*
Pan	-	**0.000**	**0.000**
Gorilla	0.238	-	**0.015**
Pongo	0.343	**0.023**	-

TABLE 7 Post hoc pairwise comparisons among great apes after Procrustes ANOVA. Results in bold are statistically significant
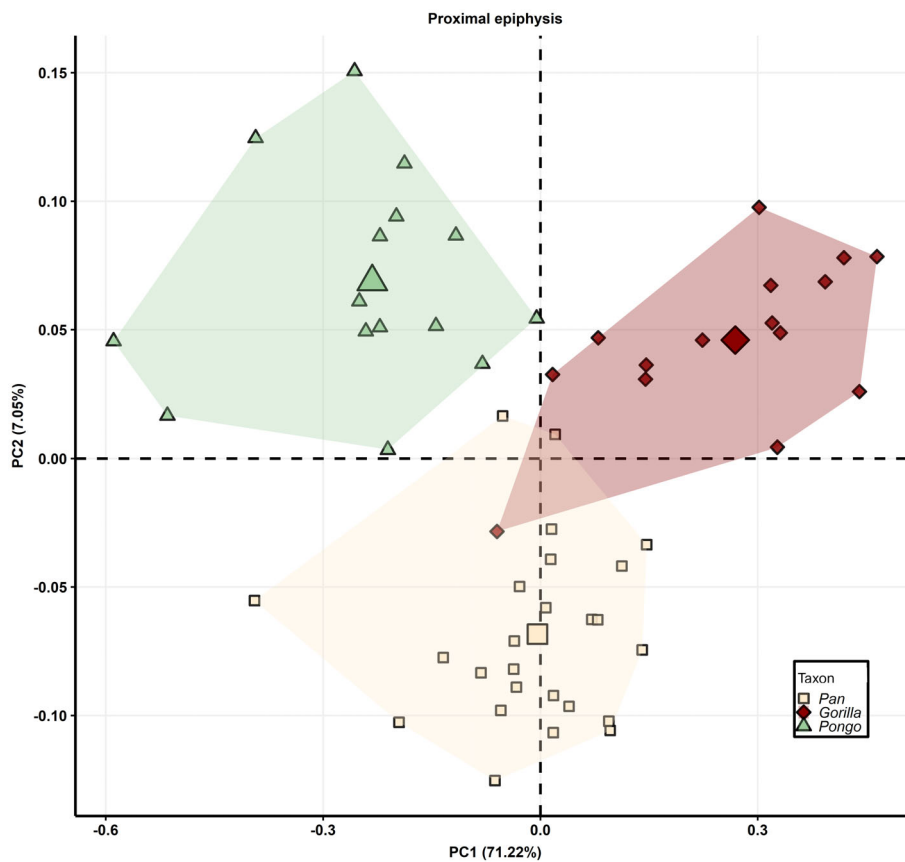
	Pan	*Gorilla*	*Pongo*
Pan	-	**0.001**	**0.001**
Gorilla		-	**0.032**
Pongo			-

dorsiflexion axis inclination at the ankle (Barnett & Napier, 1953; Ogden, 1974a, 1974b), consistent with the requirement for bipedal locomotion (Susman & Stern, 1982), but never quantified. In humans, the degree of inclination of the PTFJ surface is remarkably variable, ranging from 5° to 80° (Eichenblat & Nathan, 1983). Ogden (1974a, 1974b) found that oblique joints (>20°) have smaller articular surface areas decreasing mobility and reducing the joint ability to accommodate torsional forces, with a higher incidence (70%) of subluxation or dislocation. In contrast, in humans, the less inclined PTFJ enables greater mobility and is, therefore, less prone to injury (Alves-da-Silva et al., 2019). However, horizontal PTFJ in humans is also associated with a higher risk of osteoarthritis of the knee's medial tibiofemoral compartment. The lateral tibial plateau is more supported by a horizontal PTFJ resulting in a non-uniform settlement of the whole tibial plateau, ultimately accentuating *varus* knee as well as further knee malalignment and provoking osteoarthritis in the medial compartment (Chang et al., 2020; Huang et al., 2021).

Both these mechanisms may be related to hindlimb adaptations for obligate bipedalism in humans: the angled PTFJ observed in humans (Eichenblat & Nathan, 1983) may reflect the reduced torsional forces to which the fibula is subjected during ankle dorsiflexion in bipedality. Ankle dorsiflexion produces a posterolateral shift of the fibular head (Barnett & Napier, 1953; Ogden, 1974a, 1974b) which is, therefore, more accentuated in nonhuman apes than in humans (DeSilva, 2009; Stern & Susman, 1983). The decreased mobility of the fibula that an oblique PTFJ concurs to limiting ankle mobility, but at the same time, might cause the proximal fibula to be more prone to dislocation. A predominantly horizontal PTFJ in humans (<5%, Eichenblat & Nathan, 1983) would theoretically provide greater knee lateral stabilization in flexion and extension but would ultimately lead to joint malalignment (*varus* knee). The accentuated *varus* knee in humans contrasts the need to minimize transverse shear stresses achieved with a *valgus* knee (Tardieu & Trinkaus, 1994). The latter may be linked to the different orientations of ground reaction forces in bipedal walking in humans (more anteroposteriorly oriented) and chimpanzees (laterally oriented) (Johnson et al., 2022), also in agreement with the relative fibular gracility seen in humans compared to great apes (Marchi, 2007).

Our 3D-GM analysis reveals that the fibular head of humans has symmetrical anteroposterior and mediolateral proportions, with well-rounded but diminutive anterior and posterior projections, which anchor the respective anterior and posterior tibiofibular collateral ligaments and are located more superiorly than in great apes (Figures 2

14 | WILEY—**AMERICAN JOURNAL OF BIOLOGICAL ANTHROPOLOGY** *The Official Journal of the American Association of Biological Anthropologists*

PIETROBELLI ET AL.

FIGURE 8 Form space PCA scatterplots considering PC scores of *Pan* (yellow squares), *Gorilla* (red rhombuses) and *Pongo* (green triangles) groups and relative groups' means along the first two PCs.

and 3, Figure S3). This superior, rounded configuration may be implicated in the ligament lesion, and PTFJ dislocation mechanism Ogden (1974a, 1974c) described as the result of a sudden inversion and plantar flexion of the foot in bipedal locomotion, with simultaneous flexion of the knee and concomitant twisting of the limb, as also verified by 3D displacements analysis (Alves-da-Silva et al., 2019). Moreover, it was revealed that full extension of the knee fully recruits the APTFL (Alves-da-Silva et al., 2019), suggesting its significance for human bipedal walking on an extended hindlimb. This reduces the energy cost of locomotion compared with chimpanzees walking both quadrupedally and bipedally (Pontzer et al., 2009; Sockol et al., 2007).

The human fibular head is also characteristically surmounted by a styloid process (Figures 2 and 3, Figure S3). This feature may play a crucial role in supporting the lateral compartment of the knee when in full extension (Tardieu, 1999) since it provides attachment for the PFL to the popliteus tendon. In addition, these soft structures stabilize the whole posterolateral tendon and ligaments complex, the posterolateral corner of the knee by preventing posterior translation, *varus* angulation, and primary external rotation of the tibia relative to the femur (LaPrade et al., 2003; LaPrade & Bollom, 2001).

The morphology of the muscle attachment areas on the fibular head in humans may also reflect functional adaptations to bipedal walking. In humans, the long head of the m. *biceps femoris* inserts superiorly onto the rounded, anterolateral portion of the fibular head and expands posteriorly onto the styloid process through its interfacing components (direct arms of short and long heads, an anterior arm

of long head; LaPrade et al., 2003; LaPrade & Bollom, 2001; Figures 2 and 3, Figure S3). The role of this muscle in obligate bipedal locomotion is crucial due to its configuration within the hamstring. In humans, as the lever for the hamstrings is lengthened, the muscle moment arms (at the hip and/or knee) are shortened, decreasing the power-generating capacity of the muscles but favoring speed generation in the form of angular velocity, essential for running (Hogervorst & Vereecke, 2015; Kozma et al., 2018). It has been observed that humans possess shorter m. *biceps femoris* moment arms at the knee relative to femur length than great apes (Payne et al., 2006a; Visser et al., 1990), in agreement with the less posteroinferiorly elongated distal insertion onto the fibular head (Figures 2 and 3, Figure S3).

Concerning the fibular proximal insertion of the m. *peroneus longus*, our 3D-GM analysis shows that humans possess a relatively flat, narrow, anteriorly facing attachment, in contrast to an anterolaterally expanded concave attachment observed in great apes. In humans, peroneal muscles are active during the support phase of locomotion, similar to great apes (Jungers et al., 1993; Stern & Susman, 1983; Figures 2 and 3, Figure S3). EMG studies have shown that in humans, peroneal muscles are more active when everting the inverted foot (Bavdek et al., 2018), suggesting their essential role in laterally stabilizing the inverted ankle joint while traversing a medially inclined ramp. Peroneal muscles in humans also have been reported to form concave furrows along the anterior fibular surface of the diaphysis in correlation with a combined effect of age and mechanical loading (Chevalier & Tignères, 2020; Hagihara & Nara, 2016).

PIETROBELLI ET AL.

AMERICAN JOURNAL OF
BIOLOGICAL ANTHROPOLOGY
The Official Journal of the American Association of Biological Anthropologists

WILEY 15

While no specific studies on peroneal anatomy and electromyography were performed on great apes, previous research on human peroneal muscles activation and fibular diaphyseal anatomy (Bavdek et al., 2018; Chevalier & Tignères, 2020) allow us to suggest that the lack of a concavity in the anterior surface of the fibula is indicative of lower peroneal activity in humans than in great apes. This finding agrees with previous studies that suggested a connection between a wider peroneal groove and fossa, observed at the distal fibular extremity, and larger, powerful peroneal muscles (Marchi, 2015b; Marchi et al., 2022).

The present study also showed a proximal insertion of the m. *soleus* on the fibula that is narrower, deeper, and more posteriorly elongated in humans than in great apes (Figures 2 and 3, Figure S3). This finding is consistent with the m. *soleus* contributing to over 60% of m. *triceps surae* mass in humans (Hanna & Schmitt, 2011) and generating the central part of work/energy at the ankle joint throughout the entire stance phase of bipedal running (Bohm et al., 2021; Lai et al., 2015). The m. *triceps surae* is twice as heavy relative to human body size than in chimpanzees (Aiello & Dean, 1990; Zihlman & Brunker, 1979). It is also responsible for supporting the body weight after touchdown throughout the walking stance phase and for lifting the body's entire weight in the second half of the stance phase (Hanna & Schmitt, 2011).

4.2 | Differences among great apes

In great apes, the observed horizontal PTFJ agrees with a highly mobile articulation necessary to accommodate the high degree of ankle dorsiflexion and eversion-inversion (Ogden, 1974a, 1974b) that characterize, for example, vertical climbing (DeSilva, 2009; Holowka et al., 2017; Figures 2 and 6, Figure S5). The more horizontal PTFJ in great apes may also facilitate anteroposterior excursion of the proximal fibula proximally, as observed for humans (Scott et al., 2007). Previous studies on the kinematics of the knee joint of great apes during bipedal or quadrupedal terrestrial walking (Finestone et al., 2018; O'Neill et al., 2015) and climbing (DeSilva, 2009; Isler, 2005) did not include the PTFJ in their evaluations. However, these studies noted a consistently wider range of motion and distinctive patterns of knee and ankle flexion in great apes than in humans and specific trends within great apes. Indeed, our 3D-GM analysis results show that all great apes have a more horizontal PTFJ than humans in mean shape (Figures 2, 3, and 6, Figure S3, Figure S5). However, differences among the great apes are present. In particular, chimpanzees display a markedly horizontal PTFJ, coherent with a higher flexibility of the knee and ankle during vertical climbing (Barnett & Napier, 1952; Crompton et al., 2010; Ogden, 1974a, 1974b), while orangutans and gorillas show a more posteriorly tilted articulation. This feature in orangutans could be linked to PTFJ stabilization during knee extension while walking bipedally in an arboreal setting (Thorpe et al., 2007), similar to that observed for tilted PTFJ in humans (Eichenblat & Nathan, 1983; Ogden, 1974a, 1974b). In gorillas, kinematic data are needed to understand how this pattern may relate to specific variations of fibular excursions associated with knee and ankle movements.

However, in humans, a larger anterior displacement on the fibular head is observed with knee varus load in flexion (Scott et al., 2007). Therefore, we tentatively suggest that the orientation of the PTFJ in orangutans and gorillas may be similarly preventing anterior displacement of the fibula and be linked to their wider bicondylar angles than in chimpanzees as knee flexion increases (Lovejoy, 2007), which also mitigates lateral displacement and varus loading of the knee. This shape is consistent with a broader range of motion of thigh abduction (Isler, 2005), which may result in a mediolateral bending load increase on the fibula, acting as a lateral stabilizer, as observed in humans (Wang et al., 1996). A similar explanation may also account for the differences observed for the m. *biceps femoris* and proximal FCL insertion on the fibular head of orangutans, which are more laterally protruding and deeper than in African great apes (Figures 2 and 6, Figure S5). The fibular head is pulled posteriorly as the m. *biceps femoris* and FCL becomes taut (Semonian et al., 1995). Indeed, in humans, when the knee is semi-flexed, the m. *biceps femoris* contributes to thigh abduction and lateral rotation (LaPrade et al., 2003). Suppose a similar function is assumed for other hominids (Kumakura, 1989), a lateral bony protrusion for the m. *biceps femoris* in orangutans may be mechanically advantageous for knee extension/flexion while the thigh is laterally rotated (Isler, 2005). On the other hand, African great apes lack this feature, which may be related to the modest activity of this muscle during knuckle-walking (Kumakura, 1989).

Our results show that all great apes separate from one another (Figure 6) due to distinctive proximal fibular morphology. Previous studies found significant differences in relative (to the tibia) fibular strength (Marchi, 2007, 2015a) and distal fibular morphology (Marchi et al., 2022) among taxa that engage more frequently in vertical climbing behavior (*Pan* and *Pongo*) compared to those that are more terrestrial (*Homo* and *Gorilla*). The authors linked these differences to larger peroneal muscles in the former, a feature that has generally been associated with arboreal great apes (Aiello & Dean, 1990; McLean & Marzke, 1994; Stern & Susman, 1983). These results are supported by our study, in which orangutans show a concave and markedly anterolaterally protruding attachment area for the peroneal muscles, with an expansion best seen in the medial view. In contrast, gorillas and chimpanzees display a more anterior insertion area(Figures 2 and 6, Figure S5). As detailed above, m. *peroneus longus* is recruited for the lateral stabilization of the inverted foot (Bavdek et al., 2018) and orangutans perform extreme inversion and eversion of the foot when traversing trees (Manduell et al., 2012; Oishi et al., 2012; Thorpe et al., 2007) and when supporting themselves on horizontal branches or vertical tree trunks (Thorpe & Crompton, 2006). The anterolateral protrusion attachment of m. *peroneus longus* of orangutans may facilitate these sagittal movements by increasing the bony leverage in the lateral plane. However, to our knowledge, no empirical demonstration of this has been provided for great apes. In addition, in gorillas, this insertion also shows a mild lateral expansion that is not seen in chimpanzees. EMG studies in humans showed that this muscle's anterior neuromuscular compartment (NMC) contributed to both eversion and plantarflexion movements, whereas the posterior compartment mainly contributed to eversion only (Bakkum et al., 1996; Mendez-Rebolledo

16 | WILEY—AMERICAN JOURNAL OF BIOLOGICAL ANTHROPOLOGY *The Official Journal of the American Association of Biological Anthropologists*

PIETROBELLI ET AL.

et al., 2021). As gorillas engage in terrestrial plantigrade quadrupedalism with propulsive plantarflexion (Straus, 1940), their anteriorly protruding and moderately anterolaterally expanded attachment may be related to a greater contribution of the m. *peroneus longus* in propulsion during plantarflexion. However, the amount of arboreal locomotion varies among eastern and western gorillas (Remis, 1998). As both species were included and combined in our sample, it is difficult to test this hypothesis properly. More EMG studies are needed to frame better the contribution of peroneal muscles in great ape locomotion behavior.

Distinctive patterns among great apes are also found concerning the m. *soleus* (Figures 2 and 6, Figure S5). The 3D-GM analysis shows that all great apes possess a medially expanded insertion of m. *soleus*, which has been linked to their arborealism (Hanna & Schmitt, 2011). African great apes, however, display an inferiorly more protruding m. *soleus* and larger proximal insertion than do orangutans, in agreement with the observed greater mass of this muscle relative to the total m. *triceps surae* mass in gorillas and chimpanzees (Hanna & Schmitt, 2011). This difference may also reflect variation in muscle fiber type distribution (Myatt et al., 2011) and gross muscle anatomy (Marchi et al., 2018; Payne et al., 2006b) among great apes. In particular, it might refer to the need in African great apes for controlled mobility when arboreal and greater speed and power when terrestrial, as compared to the slow movements with a greater joint range of motions that the arboreal behavior of orangutans (Myatt et al., 2011; Thorpe et al., 1999).

A possible limitation of our study is that comparisons among genera may have been affected by differences across species within each genus, which were not addressed in our analyses due to the small sample size. For example, *Pan paniscus* and *Gorilla beringei* are represented by only 1 and 3 specimens, respectively. Indeed, further studies should test for possible differences across species within each genus and possible links to variation in locomotor behavior, as has been shown elsewhere (Doran, 1993; Harper et al., 2021; Remis, 1998).

5 | CONCLUSIONS

This study expands our understanding of leg structure and posture by providing a detailed description and assessment of proximal fibular shape variation in extant humans and great apes using 3D-GM. In addition, our study quantitatively characterized the distinctive features of the human fibular head compared to those of great apes (i.e., oblique articular surface, the presence of the styloid process, and specific morphology of muscle attachment sites), suggesting a crucial role of the fibula among functional adaptations to human obligate bipedalism.

Great apes also display distinctive features in their proximal fibular morphology, consistent with known differences in locomotor behavior. However, while some features may correlate to the higher degree of arborealism in orangutans (i.e., a laterally expanded m. *peroneus longus* insertion) or contribute to the separation of Asian and African great apes (i.e., the expansion of m. *biceps femoris* and m. *soleus* insertion),

others are distinct within each genus and might reflect specific hindlimb posture requirements for habitual locomotor behavior (i.e., the orientation of the articular surface). The results of our study provide essential details about the comparative morphology of the proximal fibula in extant hominids that should prove valuable for interpretations of fossil hominin locomotor behaviors.

AUTHOR CONTRIBUTIONS

ACKNOWLEDGMENTS

CONFLICT OF INTEREST

The authors declare no conflict of interest.

DATA AVAILABILITY STATEMENT

All data acquired and analyzed in this work is available upon reasonable request addressed to the corresponding authors. Landmarks coordinates and sample lists for geometric morphometric analysis are available in Appendix S2 and Appendix S3.

ORCID

Annalisa Pietrobelli https://orcid.org/0000-0002-2558-1118
Rita Sorrentino https://orcid.org/0000-0002-6529-7250
Damiano Marchi https://orcid.org/0000-0002-6331-8783

REFERENCES

Adams, D. C., Collyer, M. L., & Kaliontzopoulou, A. (2018). *Geomorph: Software for geometric morphometric analyses.* R Package Version *3.0.7* (Version 3.2.0).

PIETROBELLI ET AL.

AMERICAN JOURNAL OF
BIOLOGICAL ANTHROPOLOGY
The Official Journal of the American Association of Biological Anthropologists
WILEY | 17

Aiello, L. C., & Dean, M. C. (1990). *An introduction to human evolutionary anatomy*. Academic Press.

Almécija, S., Tallman, M., Alba, D. M., Pina, M., Moyà-Solà, S., & Jungers, W. L. (2013). The femur of *Orrorin tugenensis* exhibits morphometric affinities with both Miocene apes and later hominins. *Nature Communications*, 4, 2888. https://doi.org/10.1038/ncomms3888

Alves-da-Silva, T., Guerra-Pinto, F., Matias, R., & Pessoa, P. (2019). Kinematics of the proximal tibiofibular joint is influenced by ligament integrity, knee and ankle mobility: An exploratory cadaver study. *Knee Surgery, Sports Traumatology, Arthroscopy*, 27, 405–411. https://doi.org/10.1007/s00167-018-5070-8

Anavian, J., Marchetti, D. C., Moatshe, G., Slette, E. L., Chahla, J., Brady, A. W., Civitarese, D. M., & LaPrade, R. F. (2018). The forgotten joint: Quantifying the anatomy of the proximal tibiofibular joint. *Knee Surgery, Sports Traumatology, Arthroscopy*, 26, 1096–1103. https://doi.org/10.1007/s00167-017-4508-8

Andersen, K. (1985). Dislocation of the superior tibiofibular joint. *Injury*, 16, 494–498.

Bakkum, B. W., Russell, K., Adamcryck, T., & Keyes, M. (1996). Gross anatomic evidence of partitioning in the human fibularis longus and brevis muscles. *Clinical Anatomy*, 9, 381–385. https://doi.org/10.1002/(SICI)1098-2353(1996)9:6<381::AID-CA4>3.0.CO;2-E

Barnett, C. H., & Napier, J. R. (1952). The axis of rotation at the ankle joint in man; its influence upon the form of the talus and the mobility of the fibula. *Journal of Anatomy*, 86, 1–9.

Barnett, C. H., & Napier, J. R. (1953). The rotatory mobility of the fibula in eutherian mammals. *Journal of Anatomy*, 87, 11–21.

Bavdek, R., Zdolšek, A., Strojnik, V., & Dolenec, A. (2018). Peroneal muscle activity during different types of walking. *Journal of Foot and Ankle Research*, 11, 50. https://doi.org/10.1186/s13047-018-0291-0

Belcastro, M. G., Pietrobelli, A., Rastelli, E., Iannuzzi, V., Toselli, S., & Mariotti, V. (2019). Variations in epiphyseal fusion and persistence of the epiphyseal line in the appendicular skeleton of two identified modern (19th-20th c.) adult Portuguese and Italian samples. *American Journal of Physical Anthropology*, 169, 448–463. https://doi.org/10.1002/ajpa.23839

Bohm, S., Mersmann, F., Santuz, A., Schroll, A., & Arampatzis, A. (2021). Muscle-specific economy of force generation and efficiency of work production during human running. *eLife*, 10, e67182.

Bookstein, F. L. (1991). *Morphometric tools for landmark data. Geometry and biology*. Cambridge University Press.

Bozkurt, M., Yilmaz, E., Atlihan, D., Tekdemir, I., Havitçioğğlu, H., & Günal, I. (2003). The proximal tibiofibular joint. *Clinical Orthopaedics and Related Research*, 406, 136–140.

Cant, J. G. H. (1987). Positional behavior of female Bornean orangutans (*Pongo pygmaeus*). *American Journal of Primatology*, 12, 71–90. https://doi.org/10.1002/ajp.1350120104

Carleton, A. (1941). A comparative study of the inferior tibio-fibular joint. *Journal of Anatomy*, 76, 45–55.

Carlson, K. J. (2005). Investigating the form-function interface in African apes: Relationships between principal moments of area and positional behaviors in femoral and humeral diaphyses. *American Journal of Physical Anthropology*, 127, 312–334.

Chang, J., Zhu, Z., Han, W., Zhao, Y., Kwoh, C. K., Lynch, J. A., Hunter, D. J., & Ding, C. (2020). The morphology of proximal tibiofibular joint (PTFJ) predicts incident radiographic osteoarthritis: Data from osteoarthritis initiative. *Osteoarthritis and Cartilage*, 28, 208–214. https://doi.org/10.1016/j.joca.2019.11.001

Chevalier, T., & Tignères, M. (2020). Age-related site-specific modifications in diaphyseal structural properties of the human fibula: Furrows and cross-sectional geometry. *American Journal of Physical Anthropology*, 173, 535–555.

Coleman, M. N., & Colbert, M. W. (2007). Technical note: CT thresholding protocols for taking measurements on three-dimensional models. *American Journal of Physical Anthropology*, 133, 723–725. https://doi.org/10.1002/ajpa.20583

Crompton, R. H., Sellers, W. I., & Thorpe, S. K. (2010). Arboreality, terrestriality and bipedalism. *Philosophical Transactions of the Royal Society of London. Series B, Biological Sciences*, 365, 3301–3314. https://doi.org/10.1098/rstb.2010.0035

DeSilva, J. M. (2008). *Vertical climbing adaptations in the anthropoid ankle and midfoot: Implications for locomotion in Miocene catarrhines and Plio-Pleistocene hominins (Doctoral dissertation)*. University of Michigan.

DeSilva, J. M. (2009). Functional morphology of the ankle and the likelihood of climbing in early hominins. *Proceedings of the National Academy of Sciences of the United States of America*, 106, 6567–6572.

DeSilva, J. M. (2010). Revisiting the "midtarsal break". *American Journal of Physical Anthropology*, 141, 245–258.

DeSilva, J. M., Holt, K. G., Churchill, S. E., Carlson, K. J., Walker, C. S., Zipfel, B., & Berger, L. R. (2013). The lower limb and mechanics of walking in *Australopithecus sediba*. *Science*, 340, 1232999. https://doi.org/10.1126/science.1232999

DeSilva, J. M., & Throckmorton, Z. J. (2010). Lucy's flat feet: The relationship between the ankle and rearfoot arching in early hominins. *PLoS One*, 5, e14432.

Doran, D. M. (1993). Comparative locomotor behavior of chimpanzees and bonobos: The influence of morphology on locomotion. *American Journal of Physical Anthropology*, 91, 83–98.

Doran, D. M. (1996). Comparative positional behavior of the African apes. In M. C. McGrew, L. F. Marchant, & T. Nishida (Eds.), *Great ape societies* (pp. 213–224). Cambridge University Press.

Doran, D. M., & NcNeilage, A. (1993). Gorilla ecology and behavior. *Evolutionary Anthropology*, 6, 120–131. https://doi.org/10.1002/(SICI)1520-6505(1998)6:4<120::AID-EVAN2>3.0.CO;2-H

Eichenblat, M., & Nathan, H. (1983). The proximal tibiofibular joint. *International Orthopaedics*, 7, 31–39.

Evans, F. G., & Bang, S. (1966). Physical and histological differences between human fibular and femoral compact bone. In F. Gaynor Evans (Ed.), *Studies on the anatomy and function of bone and joints* (pp. 142–155). Springer.

Ferrero, E. M., Pastor, J. F., Fernandez, F. D. F., Cachorro, M. B., Diogo, R., & Wood, B. (2012). Comparative anatomy of the lower limb muscles of hominoids: Attachments, relative weights, innervation and functional morphology. In E. F. Hughes & M. E. Hill (Eds.), *Primates: Classification, evolution, and behavior* (pp. 1–69). Nova Science Publishers.

Finestone, E. M., Brown, M. H., Ross, S. R., & Pontzer, H. (2018). Great ape walking kinematics: Implications for hominoid evolution. *American Journal of Physical Anthropology*, 166, 43–55.

Frelat, M. A., Shaw, C. N., Sukhdeo, S., Hublin, J. J., Benazzi, S., & Ryan, T. M. (2017). Evolution of the hominin knee and ankle. *Journal of Human Evolution*, 108, 147–160. https://doi.org/10.1016/j.jhevol.2017.03.006

Funk, J. R., Rudd, R. W., Kerrigan, J. R., & Crandall, J. R. (2007). The line of action in the tibia during axial compression of the leg. *Journal of Biomechanics*, 40, 2277–2282. https://doi.org/10.1016/j.jbiomech.2006.10.012

Gunz, P., & Mitteroecker, P. (2013). Semilandmarks: A method for quantifying curves and surfaces. *Hystrix*, 24, 103–109. https://doi.org/10.4404/hystrix-24.1-6292

Gunz, P., Mitteroecker, P., & Bookstein, F. L. (2006). Semilandmarks in three dimensions. In D. E. Slice (Ed.), *Modern morphometrics in physical anthropology* (1st ed., pp. 73–98). Springer Science & Business Media.

Hagihara, Y., & Nara, T. (2016). Morphological features of the fibula in Jomon hunter-gatherers from the shell mounds of the Pacific coastal area. *American Journal of Biological Anthropology*, 160(4), 708–718. doi:10.1002/ajpa.23000

Hanna, J. B., & Schmitt, D. (2011). Comparative triceps surae morphology in primates: A review. *Anatomy Research International*, 2011, 191509. https://doi.org/10.1155/2011/191509

Harcourt-Smith, W. E. H. (2015). Origin of bipedal locomotion. In W. Henke & I. Tattersall (Eds.), *Handbook of paleoanthropology* (pp. 1919–1959). Springer. https://doi.org/10.1007/978-3-642-39979-4_48

Harcourt-Smith, W. E. H., & Aiello, L. C. (2004). Fossils, feet and the evolution of bipedal locomotion. *Journal of Anatomy, 204*, 403–416.

Harcourt-Smith, W. E. H., Tallman, M., Frost, S., Wiley, D., Rohlf, F. J., & Delson, E. (2008). Analysis of selected hominoid joint surfaces using laser scanning and geometric morphometrics: A preliminary report. In E. Sargis & M. Dagosto (Eds.), *Mammalian evolutionary morphology* (pp. 373–383). Springer.

Harmon, E. (2007). The shape of the hominoid proximal femur: A geometric morphometric analysis. *Journal of Anatomy, 210*, 170–185.

Harmon, E. (2009). Size and shape variation in the proximal femur of *Australopithecus africanus. Journal of Human Evolution, 56*, 551–559.

Harmon, E. H. (2006). Size and shape variation in Australopithecus afarensis proximal femora. *Journal of Human Evolution, 51*, 217–227.

Harper, C. M., Ruff, C. B., & Sylvester, A. D. (2021). Gorilla calcaneal morphological variation and ecological divergence. *American Journal of Biological Anthropology, 174*, 49–65.

Heaton, J. L., Pickering, T. R., Carlson, K. J., Crompton, R. H., Jashashvili, T., Beaudet, A., Bruxelles, L., Kuman, K., Heile, A. J., Stratford, D., & Clarke, R. J. (2019). The long limb bones of the StW 573 *Australopithecus* skeleton from Sterkfontein member 2: Descriptions and proportions. *Journal of Human Evolution, 133*, 167–197. https://doi.org/10.1016/j.jhevol.2019.05.015

Hogervorst, T., & Vereecke, E. E. (2015). Evolution of the human hip. Part 2: Muscling the double extension. *Journal of Hip Preservation Surgery, 2*(1), 3–14.

Holowka, N. B., O'Neill, M. C., Thompson, N. E., & Demes, B. (2017). Chimpanzee ankle and foot joint kinematics: Arboreal versus terrestrial locomotion. *American Journal of Physical Anthropology, 164*, 131–147. https://doi.org/10.1002/ajpa.23262

Huang, C., Chen, S., Liu, D., Lu, Z., Cheng, J., Li, Z., Chen, Y., Yan, Z., Zhu, Q., & Du, T. (2021). Association between the inclination angle of the proximal tibiofibular joint surface and medial compartment knee osteoarthritis. *Annals of Palliative Medicine, 10*, 8753–8761. https://doi.org/10.21037/apm-21-1348

Isler, K. (2005). 3D-kinematics of vertical climbing in hominoids. *American Journal of Physical Anthropology, 126*, 66–81. https://doi.org/10.1002/ajpa.10419

Javois, C., Tardieu, C., Lebel, B., Seil, R., & Hulet, C. (2009). Comparative anatomy of the knee joint: Effects on the lateral meniscus. *Orthopaedics & Traumatology: Surgery & Research, 95*, 49–59.

Johnson, R. T., O'Neill, M. C., & Umberger, B. R. (2022). The effects of posture on the three-dimensional gait mechanics of human walking in comparison with walking in bipedal chimpanzees. *The Journal of Experimental Biology, 225*, jeb243272. https://doi.org/10.1242/jeb.243272

Jungers, W. L., Larson, S. G., Harcourt-Smith, W. E., Morwood, M. J., Sutikna, T., Due Awe, R., & Djubiantono, T. (2009). Descriptions of the lower limb skeleton of *Homo floresiensis. Journal of Human Evolution, 57*, 538–554.

Jungers, W. L., Meldrum, D. J., & Stern, J. T., Jr. (1993). The functional and evolutionary significance of the human peroneus tertius muscle. *Journal of Human Evolution, 25*, 377–386.

Kaplan, E. B. (1957). Surgical approach to the lateral (peroneal) side of the knee joint. *Surgery Gynecology and Obstetrics, 104*, 346–356.

Kaseda, M., Nakamura, M., Ichihara, N., Hayakawa, T., & Asari, M. (2008). A macroscopic examination of m. biceps femoris and m. gluteus maximus in the orangutan. *The Journal of Veterinary Medical Science, 70*, 217–222. https://doi.org/10.1292/jvms.70.217

Klingenberg, C. P. (2016). Size, shape, and form: Concepts of allometry in geometric morphometrics. *Development Genes and Evolution, 226*, 113–137. https://doi.org/10.1007/s00427-016-0539-2

Kozma, E. E., Webb, N. M., Harcourt-Smith, W., Raichlen, D. A., D'Août, K., Brown, M. H., Finestone, E. M., Ross, S. R., Aerts, P., & Pontzer, H. (2018). Hip extensor mechanics and the evolution of walking and climbing capabilities in humans, apes, and fossil hominins. *Proceedings of the National Academy of Sciences of the United States of America, 115*, 4134–4139. https://doi.org/10.1073/pnas.1715120115

Kumakura, H. (1989). Functional analysis of the biceps femoris muscle during locomotor behavior in some primates. *American Journal of Physical Anthropology, 79*, 379–391.

Lai, A., Lichtwark, G. A., Schache, A. G., Lin, Y. C., Brown, N. A., & Pandy, M. G. (2015). In vivo behavior of the human soleus muscle with increasing walking and running speeds. *Journal of Applied Physiology, 118*, 1266–1275.

Lambert, K. L. (1971). The weight-bearing function of the fibula: A strain gauge study. *Journal of Bone & Joint Surgery, 53*, 507–513.

LaPrade, R. F., & Bollom, T. S. (2001). Anatomy and biomechanics of the posterolateral aspect of the knee. In G. C. Fanelli (Ed.), *Posterior cruciate ligament injuries* (pp. 23–46). Springer. https://doi.org/10.1007/978-0-387-21601-0_2

LaPrade, R. F., Ly, T. V., Wentorf, F. A., & Engebretsen, L. (2003). The posterolateral attachments of the knee. *The American Journal of Sports Medicine, 31*, 854–860.

Latimer, B., Ohman, J. C., & Lovejoy, C. O. (1987). Talocrural joint in African hominoids: Implications for *Australopithecus afarensis. American Journal of Physical Anthropology, 74*, 155–175.

Lovejoy, C. O. (2007). The natural history of human gait and posture. Part 3. The Knee. *Gait & Posture, 25*, 325–341. https://doi.org/10.1016/j.gaitpost.2006.05.001

Manduell, K. L., Harrison, M. E., & Thorpe, S. K. S. (2012). Forest structure and support availability influence orangutan locomotion in Sumatra and Borneo. *American Journal of Primatology, 74*, 1128–1142. https://doi.org/10.1002/ajp.22072

Marchi, D. (2007). Relative strength of the tibia and fibula and locomotor behavior in hominoids. *Journal of Human Evolution, 53*, 647–655.

Marchi, D. (2015a). Variation in tibia and fibula diaphyseal strength and its relationship with arboreal and terrestrial locomotion: Extending the investigation to non-hominoid primates. *Journal of Anthropological Sciences, 93*, 1–4.

Marchi, D. (2015b). Using the morphology of the hominoid distal fibula to interpret arboreality in *Australopithecus afarensis. Journal of Human Evolution, 85*, 136–148.

Marchi, D., Harper, C. M., Chirchir, H., & Ruff, C. B. (2019). Relative fibular strength and locomotor behavior in KNM-WT 15000 and OH 35. *Journal of Human Evolution, 131*, 48–60. https://doi.org/10.1016/j.jhevol.2019.02.005

Marchi, D., Leischner, C. L., Pastor, F., & Hartstone-Rose, A. (2018). Leg muscle architecture in primates and its correlation with locomotion patterns. *The Anatomical Record, 301*, 515–527. https://doi.org/10.1002/ar.23747

Marchi, D., Rimoldi, A., García-Martínez, D., & Bastir, M. (2022). Morphological correlates of distal fibular morphology with locomotion in great apes, humans, and *Australopithecus afarensis. American Journal of Biological Anthropology, 178*, 286–300. https://doi.org/10.1002/ajpa.24507

Martin, R., & Saller, K. (1959). *Lehrbuch der Anthropologie in systematischer Darstellung mit besonderer Berücksichtigung der anthropologischen Methoden* (Vol. 2). G. Fischer.

Martini, F., Timmons, M. J., & Tallitsch, R. B. (2009). *Human anatomy*. Pearson Benjamin Cummings.

Marzke, M. W., Longhill, J. M., & Rasmussen, S. A. (1988). Gluteus maximus muscle function and the origin of hominid bipedality. *American Journal of Physical Anthropology, 77*(4), 519–528. https://doi.org/10.1002/ajpa.1330770412

McLean, S. P., & Marzke, M. (1994). Functional significance of the fibula: Contrast between humans and chimpanzees. *Folia Primatologica, 63*, 107–114. https://doi.org/10.1159/000156802

Melchionna, M., Profico, A., Castiglione, S., Sansalone, G., Serio, C., Mondanaro, A., Di Febbraro, M., Rook, L., Pandolfi, L., Di Vincenzo, F., Manzi, G., & Raia, P. (2020). From smart apes to human brain boxes. A

PIETROBELLI ET AL.

AMERICAN JOURNAL OF
BIOLOGICAL ANTHROPOLOGY
The Official Journal of the American Association of Biological Anthropologists

WILEY | 19

uniquely derived brain shape in late hominins clade. *Frontiers in Earth Science*, 8, 273.

Mendez-Rebolledo, G., Guzmán-Venegas, R., Valencia, O., & Watanabe, K. (2021). Contribution of the peroneus longus neuromuscular compartments to eversion and plantarflexion of the ankle. *PLoS One*, 16, e0250159. https://doi.org/10.1371/journal.pone.0250159

Myatt, J. P., Schilling, N., & Thorpe, S. K. (2011). Distribution patterns of fibre types in the triceps surae muscle group of chimpanzees and orangutans. *Journal of Anatomy*, 218, 402–412.

Nagano, A., Umberger, B. R., Marzke, M. W., & Gerritsen, K. G. (2005). Neuromusculoskeletal computer modeling and simulation of upright, straight-legged, bipedal locomotion of *Australopithecus afarensis* (AL 288-1). *American Journal of Physical Anthropology*, 126(1), 2–13. https://doi.org/10.1002/ajpa.10408

O'Connell, A. L. (1958). Electromyographic study of certain leg muscles during movements of the free foot and during standing. *American Journal of Physical Medicine & Rehabilitation*, 37, 289–301.

Ogden, J. A. (1974a). Subluxation and dislocation of the proximal tibiofibular joint. *Journal of Bone & Joint Surgery*, 56, 145–154.

Ogden, J. A. (1974b). The anatomy and function of the proximal tibiofibular joint. *Clinical Orthopaedics and Related Research*, 101, 186–191.

Ogden, J. A. (1974c). Subluxation of the proximal tibiofibular joint. *Clinical Orthopaedics and Related Research*, 101, 192–197.

Oishi, M., Ogihara, N., Endo, H., Une, Y., Ichihara, N., Asari, M., & Amasaki, H. (2012). Muscle dimensions of the foot in the orangutan and the chimpanzee. *Journal of Anatomy*, 221(4), 311–317. https://doi.org/10.1111/j.1469-7580.2012.01545.x

O'Neill, M. C., Lee, L. F., Demes, B., Thompson, N. E., Larson, S. G., Stern, J. T., Jr., & Umberger, B. R. (2015). Three-dimensional kinematics of the pelvis and hind limbs in chimpanzee (*Pan troglodytes*) and human bipedal walking. *Journal of Human Evolution*, 86, 32–42.

Pasque, C., Noyes, F. R., Gibbons, M., Levy, M., & Grood, E. (2003). The role of the popliteofibular ligament and the tendon of popliteus in providing stability in the human knee. *The Journal of Bone and Joint Surgery*, 85, 292–298. https://doi.org/10.1302/0301-620x.85b2.12857

Payne, R. C., Crompton, R. H., Isler, K., Savage, R., Vereecke, E. E., Günther, M. M., & D'Août, K. (2006a). Morphological analysis of the hindlimb in apes and humans. I. Muscle architecture. *Journal of Anatomy*, 208, 709–724.

Payne, R. C., Crompton, R. H., Isler, K., Savage, R., Vereecke, E. E., Günther, M. M., & D'Août, K. (2006b). Morphological analysis of the hindlimb in apes and humans. II. Moment arms. *Journal of Anatomy*, 208, 725–742.

Pietrobelli, A., Sorrentino, R., Notariale, V., Durante, S., Benazzi, S., Marchi, D., & Belcastro, M. G. (2022). Comparability of skeletal fibulae surfaces generated by different source scanning (dual-energy CT scan vs. high resolution laser scanning) and 3D geometric morphometric validation. *Journal of Anatomy*, 241(3), 667–682. https://doi.org/10.1111/joa.13714

Pontzer, H., Raichlen, D. A., & Sockol, M. D. (2009). The metabolic cost of walking in humans, chimpanzees, and early hominins. *Journal of Human Evolution*, 56, 43–54.

Prejzner-Morawska, A., & Urbanowicz, M. (1981). Morphology of some of the lower limb muscles in primates. In A. B. Chiarelli & R. S. Corruccini (Eds.), *Primate evolutionary biology. Proceedings in life sciences* (pp. 60–67). Springer. https://doi.org/10.1007/978-3-642-68251-3_7

Preuschoft, H. (1971). Die mechanische Beanspruchung der Fibula bei Primaten. *Gegenbaurs Morphologisches Jahrbuch*, 117, 211–216.

Profico, A., Buzi, C., Castiglione, S., Melchionna, M., Piras, P., Veneziano, A., & Raia, P. (2021). Arothron: An R package for geometric morphometric methods and virtual anthropology applications. *American Journal of Physical Anthropology*, 176, 144–151. https://doi.org/10.1002/ajpa.24340

R Core Team. (2020). *R: A language and environment for statistical computing*. R Foundation for Statistical Computing https://www.R-project.org/

Reeser, L. A., Susman, R. L., & Stern, J. T. (1983). Electromyographic studies of the human foot: Experimental approaches to hominid evolution. *Foot & Ankle International*, 3(6), 391–407.

Remis, M. J. (1995). Effects of body size and social context on the arboreal activities of lowland gorillas in the Central African Republic. *American Journal of Physical Anthropology*, 97, 413–433. https://doi.org/10.1002/ajpa.1330970408

Remis, M. J. (1998). The gorilla paradox. In E. Strasser, J. G. Fleagle, A. L. Rosenberger, & H. M. McHenry (Eds.), *Primate Locomotion* (pp. 95–106). Springer. https://doi.org/10.1007/978-1-4899-0092-0_6

Rohlf, F. J., & Slice, D. (1990). Extensions of the Procrustes method for the optimal superimposition of landmarks. *Systematic Zoology*, 39, 40–59. https://doi.org/10.2307/2992207

Sammarco, G., & Mangone, P. (2000). Diagnosis and treatment of peroneal tendon injuries. *Foot and Ankle Surgery*, 6, 197–205. https://doi.org/10.1046/j.1460-9584.2000.00212.x

Sarma, A., Borgohain, B., & Saikia, B. (2015). Proximal tibiofibular joint: Rendez-vous with a forgotten articulation. *Indian Journal of Orthopaedics*, 49, 489–495. https://doi.org/10.4103/0019-5413.164041

Scarciolla, L., Herteleer, M., Turquet, E., Badr, S., Demondion, X., Jacques, T., & Cotten, A. (2021). Anatomical study of the proximal tibiofibular ligaments using ultrasound. *Insights into Imaging*, 12, 27. https://doi.org/10.1186/s13244-021-00965-z

Schlager, S. (2017). Morpho and Rvcg—Shape analysis in R. In G. Zheng, S. Li, & G. Szekely (Eds.), *Statistical shape and deformation analysis* (pp. 217–256). Academic Press.

Scott, J., Lee, H., Barsoum, W., & van den Bogert, A. J. (2007). The effect of tibiofemoral loading on proximal tibiofibular joint motion. *Journal of Anatomy*, 211, 647–653. https://doi.org/10.1111/j.1469-7580.2007.00803.x

Semonian, R. H., Denlinger, P. M., & Duggan, R. J. (1995). Proximal tibiofibular subluxation relationship to lateral knee pain: A review of proximal tibiofibular joint pathologies. *Journal of Orthopaedic & Sports Physical Therapy*, 21, 248–257.

Slice, D. E. (2006). *Modern morphometrics in physical anthropology* (1st ed.). Springer.

Sockol, M. D., Raichlen, D. A., & Pontzer, H. (2007). Chimpanzee locomotor energetics and the origin of human bipedalism. *Proceedings of the National Academy of Sciences of the United States of America*, 104, 12265–12269. https://doi.org/10.1073/pnas.0703267104

Song, Y., Xiong, Y., Chen, W., Zuo, F., Tan, L., Yao, J., Chen, N., Bleys, R., Hu, X., Zhang, S., & Wu, Y. (2018). Sectional anatomy and three-dimensional visualization of the posterolateral complex of the knee joint based on undeformed high-resolution sectional anatomical images. *The Anatomical Record*, 301, 1764–1773. https://doi.org/10.1002/ar.23926

Song, Y., Xiong, Y., Yao, J., Wang, H., Tan, L., Hu, X., Zhang, S., & Wu, Y. (2020). Applied anatomy and three-dimensional visualization of the tendon-bone junctions of the knee joint posterolateral complex. *Annals of Anatomy. Anatomischer Anzeiger*, 229, 151413. https://doi.org/10.1016/j.aanat.2019.151413

Sorrentino, R., Carlson, K. J., Bortolini, E., Minghetti, C., Feletti, F., Fiorenza, L., Frost, S., Jashashvili, T., Parr, W., Shaw, C., Su, A., Turley, K., Wroe, S., Ryan, T. M., Belcastro, M. G., & Benazzi, S. (2020). Morphometric analysis of the hominin talus: Evolutionary and functional implications. *Journal of Human Evolution*, 142, 102747. https://doi.org/10.1016/j.jhevol.2020.102747

Sorrentino, R., Stephens, N. B., Carlson, K. J., Figus, C., Fiorenza, L., Frost, S., Harcour-Smith, W., Parr, W., Saers, J., Turley, K., Wroe, S., Belcastro, M. G., Ryan, T. M., & Benazzi, S. (2020). The influence of mobility strategy on the modern human talus. *American Journal of Physical Anthropology*, 171, 456–469. https://doi.org/10.1002/ajpa.23976

Spoor, C. F., Zonneveld, F. W., & Macho, G. A. (1993). Linear measurements of cortical bone and dental enamel by computed tomography:

Applications and problems. *American Journal of Physical Anthropology*, *91*, 469–484. https://doi.org/10.1002/ajpa.1330910405

Stern, J. T., & Susman, R. L. (1983). The locomotor anatomy of *Australopithecus afarensis*. *American Journal of Physical Anthropology*, *60*, 279–317.

Straus, W. L., Jr. (1940). The posture of the great ape hand in locomotion, and its phylogenetic implications. *American Journal of Physical Anthropology*, *27*, 199–207.

Susman, R. L., & Stern, J. T. (1982). Functional morphology of *Homo habilis*. *Science*, *217*, 931–934. https://doi.org/10.1126/science.217.4563.931

Sylvester, A. D. (2013). A geometric morphometric analysis of the medial tibial condyle of African hominids. *The Anatomical Record*, *296*, 1518–1525.

Sylvester, A. D., & Pfisterer, T. (2012). Quantifying lateral femoral condyle ellipticalness in chimpanzees, gorillas, and humans. *American Journal of Physical Anthropology*, *149*, 458–467.

Takahashi, H., Tajima, G., Kikuchi, S., Yan, J., Kamei, Y., Maruyama, M., Sugawara, A., Saigo, T., & Doita, M. (2017). Morphology of the fibular insertion of the posterolateral corner and biceps femoris tendon. *Knee Surgery, Sports Traumatology, Arthroscopy*, *25*, 184–191. https://doi.org/10.1007/s00167-016-4304-x

Tardieu, C. (1981). Morpho-functional analysis of the articular surfaces of the knee-joint in primates. In A. B. Chiarelli & R. S. Corruccini (Eds.), *Primate evolutionary biology. Proceedings in life sciences* (pp. 68–80). Springer.

Tardieu, C. (1999). Ontogeny and phylogeny of femoro-tibial characters in humans and hominid fossils: Functional influence and genetic determinism. *American Journal of Physical Anthropology*, *110*, 365–377.

Tardieu, C., & Trinkaus, E. (1994). Early ontogeny of the human femoral bicondylar angle. *American Journal of Physical Anthropology*, *95*, 183–195. https://doi.org/10.1002/ajpa.1330950206

Thorpe, S. K., Crompton, R. H., Guenther, M. M., Ker, R. F., & McNeill, A. R. (1999). Dimensions and moment arms of the hind-and forelimb muscles of common chimpanzees (*Pan troglodytes*). *American Journal of Physical Anthropology*, *110*, 179–199.

Thorpe, S. K., Holder, R. L., & Crompton, R. H. (2007). Origin of human bipedalism as an adaptation for locomotion on flexible branches. *Science*, *316*, 1328–1331. https://doi.org/10.1126/science.1140799

Thorpe, S. K. S., & Crompton, R. H. (2006). Orangutan positional behavior and the nature of arboreal locomotion in Hominoidea. *American Journal of Physical Anthropology*, *131*, 384–401. https://doi.org/10.1002/ajpa.20422

Trinkaus, E. (1983). *Shanidar Neandertals*. Academic Press.

Turley, K., Guthrie, E., & Frost, S. (2011). Geometric morphometric analysis of tibial shape and presentation among catarrhine taxa. *The Anatomical Record*, *294*, 217–230.

Turley, K., White, F. J., & Frost, S. R. (2015). Phenotypic plasticity: The impact of habitat and behavior (substrate use) on adult talo-crural appositional articular joint shape both between and within closely related hominoid species. *Human Evolution*, *30*, 49–67. https://doi.org/10.14673/HE201512002

Tuttle, R. H., & Watts, D. P. (1985). The positional behavior and adaptive complexes of *Pan gorilla*. In S. Kondo (Ed.), *Primate morphophysiology, locomotor analysis and human bipedalism* (pp. 261–288). Tokyo University Press.

Venkataraman, V. V., Kraft, T. S., & Dominy, N. J. (2013). Tree climbing and human evolution. *Proceedings of the National Academy of Sciences of the United States of America*, *110*, 1237–1242.

Visser, J. J., Hoogkamer, J. E., Bobbert, M. F., & Huijing, P. A. (1990). Length and moment arm of human leg muscles as a function of knee and hip-joint angles. *European Journal of Applied Physiology and Occupational Physiology*, *61*, 453–460.

Wang, Q., Whittle, M., Cunningham, J., & Kenwright, J. (1996). Fibula and its ligaments in load transmission and ankle joint stability. *Clinical Orthopaedics and Related Research*, *330*, 261–270.

White, T. D., Black, M. T., & Folkens, P. A. (2011). *Human osteology* (3rd ed.). Academic Press.

Zeng, S. X., Wu, G. S., Dang, R. S., Dong, X. L., Li, H. H., Wang, J. F., Liu, J., Wang, D., Huang, H. L., & Guo, X. D. (2011). Anatomic study of popliteus complex of the knee in a Chinese population. *Anatomical Science International*, *86*, 213–218. https://doi.org/10.1007/s12565-011-0112-z

Zihlman, A. L., & Brunker, L. (1979). Hominid bipedalism: Then and now. *Yearbook of Physical Anthropology*, *22*, 132–162.

SUPPORTING INFORMATION

Additional supporting information can be found online in the Supporting Information section at the end of this article.